Investigating the effects of terminal alkyl chain alterations on the ODBP liquid crystal molecule

By

Ed Vinis

A dissertation submitted in partial fulfillment
of the degree requirements for the degree of

Bachelor of Science

University of Puget Sound
Department of Chemistry
Advisor: Dr. Eric Scharrer

2014

Investigating the effects of terminal alkyl chain alterations on the ODBP liquid crystal molecule

Ed Vinis

Abstract

The nematic liquid crystal phase is a very fluid phase that has the potential to be used in electronic devices efficiently. It can possess a difficult to access but very promising biaxial nematic phase which would allow for faster switching times and be less energy consuming. However, the nematic phase is normally only accessible at high temperatures (200°C), and the biaxial nematic phase has only been found in very specific compounds.

This research focuses on altering the oxadiazole bisphenol (ODBP) liquid crystal molecule which has exhibited the biaxial nematic phase. The goal of this research is to access the nematic phase at lower temperatures. This research investigated altering the terminal alkyl chain lengths on the molecule with carbon lengths C5-C10 as slight structural variations on the molecule have shown drastic changes in phase behavior. We found that shorter chain lengths possessed lower onset nematic temperatures but the middle length derivatives, C7 and C8, remained the most fluid at low temperatures. As the chains got longer, the range at which the nematic appeared became shorter.

Approved by Eric Scharrer

Table of Contents

Introduction

Liquid crystals are compounds that exhibit an intermediate phase between solid and liquid. Unlike fully solid compounds, thermotropic liquid crystals can be heated first from the organized solid phase to a semi-organized liquid crystal phase, and then to the disorganized liquid (isotropic) phase (Figure 1)[1].

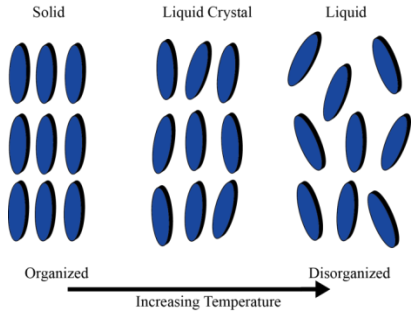

Figure 1. Order of the states of matter.

While in this mesophase, an electric current can be used to control the orientation of the molecules. This changes the way light interacts with the substance which can be very useful for many electronic devices including LCD screens (which are used in cell phones, computer/TV screens, calculators etc).

There are multiple different kinds of liquid crystal phases; some common ones include the nematic, smectic A, and smectic C phases. The nematic phase is the most fluid and disorganized making it the most practical for electronic uses[1]. In 1970, M.J. Freiser theorized that certain nematic phases had not only a single (major) axis with which they could be oriented, but also contained a perpendicular (minor) axis (Figure 2)[2]. From this theory, it was proposed that by redirecting the molecules around the minor axis, less energy would be consumed and faster switching times could be achieved.

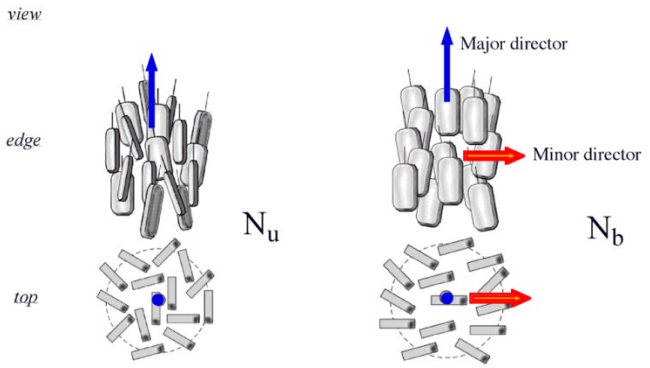

Figure 2. Uniaxial and Biaxial Nematic Phase respectively.

Compounds that possessed this biaxial nematic phase (N_b) became highly sought after and many attempts were made to synthesize such compounds[3]. It was not until 2004 that the Samulski Group at the University of North Carolina developed compounds with an oxadiazole bisphenol (ODBP) core that displayed this biaxial nematic phase[4,5]. Electro-optic studies found that faster switching times were possible for this phase[6], however this compound did not form the nematic phase until close to 200°C—useless for electronic implementation (Figure 3).

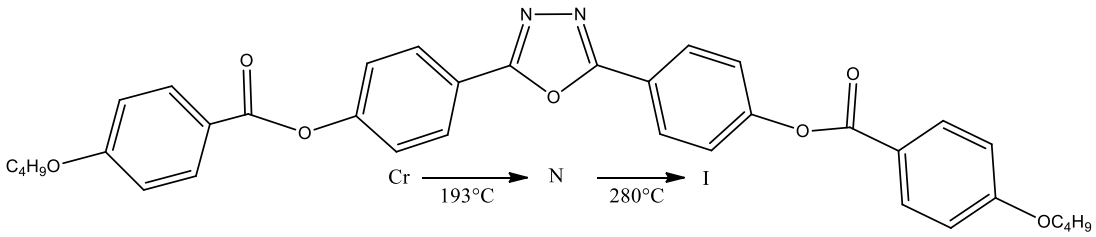

Figure 3. Phase Behavior of the unsubstituted ODBP derivative.
(Cr = crystalline, N = nematic, I = isotropic liquid)

Previous research has found that very small structural modifications resulted in significant changes in phase behavior[7,8]. Professor Eric Scharrer has been working in collaboration with the Samulski group to find ideal variations for the ODBP derivatives. The overall goal is to create a liquid crystal with a very low melting point that would allow the operating range to remain at room temperature—while retaining the N_b phase. This is very

difficult because only a small number of compounds actually exhibit this N_b phase versus the more common nematic phase. Lateral methyl groups on the benzene rings can lower the phase transition temperature significantly, by altering ways in which the molecules pack together[9]. With certain derivatives the melting temperature will not only be lowered, but upon cooling can stay in the nematic phase all the way to room temperature (Figure 4)[10].

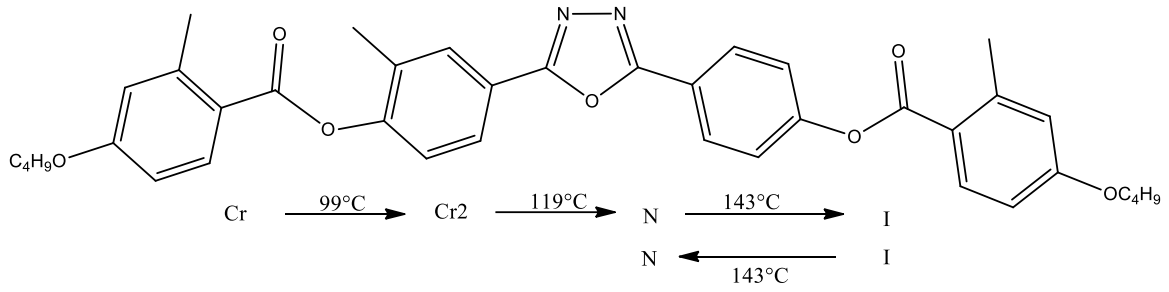

Figure 4. Phase behavior of butoxy trimethylated ODBP derivative.

More recently, Professor Scharrer has experimented with the addition of a halogen to an inner benzene ring. This supercooled in the nematic phase to room temperature, but the phase lost fluidity at lower temperatures.[10] Fluidity is an important characteristic of the nematic phase as the phase must be fluid in order to undergo electro-optic switching. As seen in Figure 5, a brominated derivative was able to access the nematic phase at low temperatures and observations show that it was able to retain fluidity at these temperatures.[10]

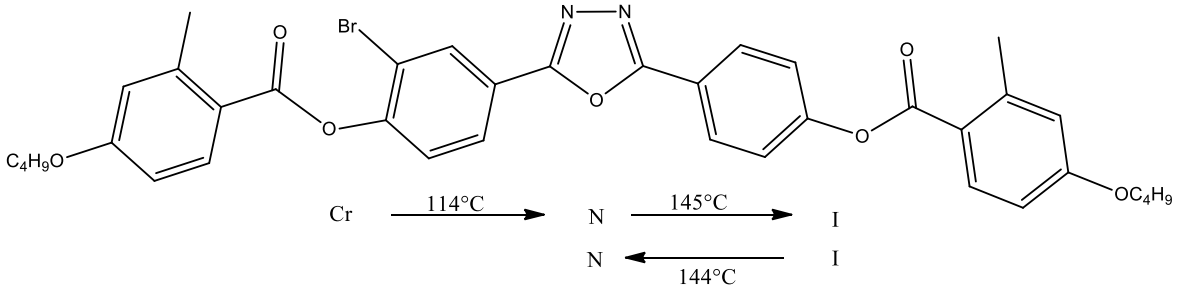

Figure 5. Phase behavior of butoxy ODBP derivative with bromine.

The goal of my research was to investigate the phase behavior of the brominated ODBP derivative with terminal alkyl chains of varying length. The hope was that by adding carbon

chains of length C5-C10, room temperature nematic phases could be reached that maintained fluidity to low temperatures.

Results and Discussion

I. Synthesis

The six ODBP liquid crystals were synthesized according to Scheme 1, following closely the procedures from previous research[10]. 3-Bromo-4-hydroxybenzoic acid was reacted with 4-hydroxybenzhydrazide in the presence of ethyl dimethylaminopropyl carbodiimide hydrochloride (EDC HCl) to form 4-Hydroxy-3-bromo-*N*-(4-hydroxybenzoyl) benzhydrazide **2**. ^{1}H-NMR analysis revealed a successful coupling and a recrystallization was performed. After a ring closure with thionyl chloride to form **3**, the complete bisphenol core was reacted with the appropriate benzoic acid **4** in the presence of EDC and DMAP to give the target compounds, **5**. The appropriate benzoic acids are not commercially available and must by synthesized separately. The resulting target compounds, **5**, were then purified by flash chromatography and recrystallization.

Scheme 1. Overall synthesis for ODBP target compounds.

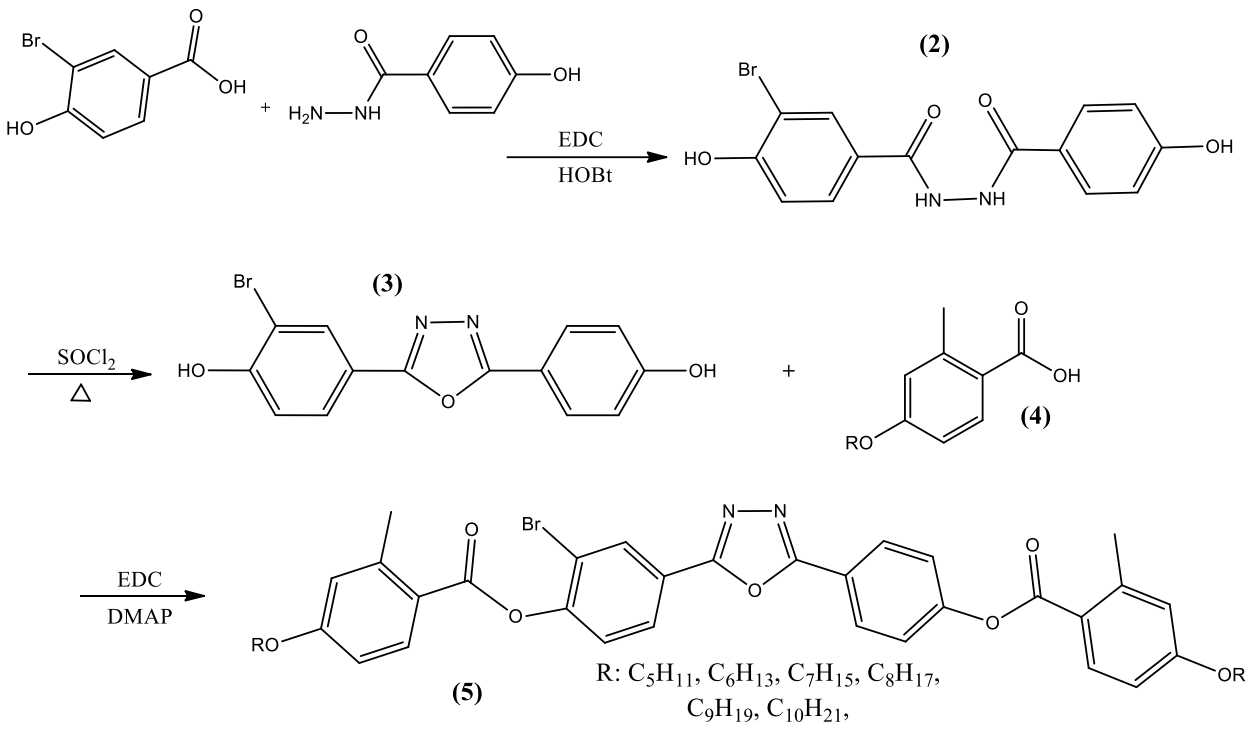

The benzoic acid derivatives, **4**, were prepared according to Scheme 2. First, 4-hydroxy-2-methylbenzoic acid was reacted with ethanol and concentrated sulfuric acid to produce ethyl 4-hydroxy-2-methyl benzoate. The phenol was alkylated using the appropriate alkyl halide to produce the different carbon length benzoic acids, C5-C10. This was followed by a basic ester hydrolysis and then acidification. All of the target compounds **5** and benzoic acid derivatives **4** have percent yields summarized in Table 1.

Scheme 2. Synthesis for desired benzoic acid derivative **4**.

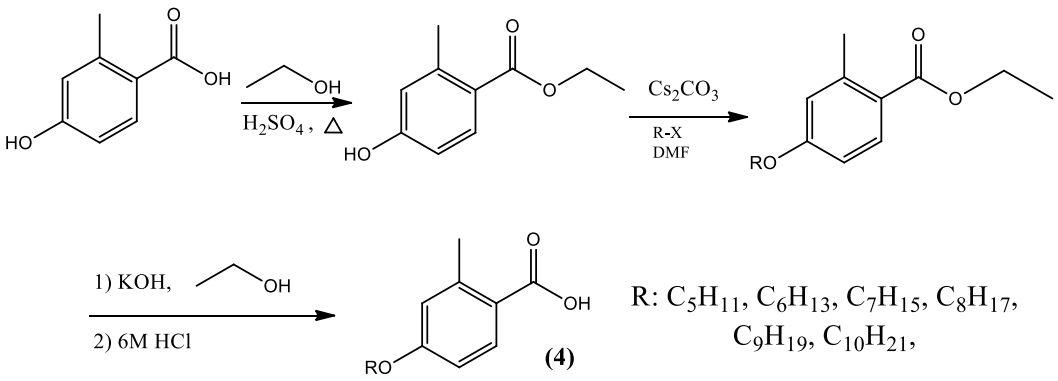

Benzoic Acid Derivatives

The synthesis of 4-pentoxy-2-methyl benzoic acid required two separate attempts both consisting of alkylation and hydrolysis. The first attempt gave a final yield of 21.66%. ^{1}H-NMR spectra revealed that most of the product loss had occurred in the hydrolysis step as the ethyl ester appeared to not be fully hydrolyzed. When repeated, the total yield was still only 32.69% but yielded enough product for coupling with the bisphenol core.

The first two attempts to prepare 4-hexyloxy-2-methyl benzoic acid had very low yields. A third attempt was much more successful and yielded enough to continue with the target synthesis. Instead of the reflux method used for the hydrolysis of the ester, this reaction was performed using a microwave reactor (140°C for 7 minutes) which sped up the process.

The synthesis of the heptyloxy benzoic acid yielded 22.4% overall but 74.15% for the hydrolysis step, revealing most of the product loss occurred in the alkylation step. An alternate method was performed in this hydrolysis where the reactant was stirred overnight at room temperature with ethanol and 2M KOH to produce the benzoate.

The synthesis of 4-octyloxy-2-methyl benzoic acid was performed in a one pot reaction with the hydrolysis taking place immediately after the alkylation step. The hydrolysis used the same method as the OC7 hydrolysis, however when analyzed by ^{1}H-NMR, the product didn't look fully hydrolyzed. Therefore the crude product was refluxed with ethanol and KOH for three hours to give a product that showed a clean ^{1}H-NMR spectrum. 4-Nonyloxy-2-methyl benzoic acid and the 4-decaloxy-2-methyl benzoic acid were also prepared by the same method.

Table 1. Summary of yields for target compounds **5** and alkoxy benzoic acids **4**.

Carbon chain derivative	**(5)**	**(4)**
OC5	19.19%	32.69%
OC6	24.39%	34.30%
OC7	18.42%	22.40%
OC8	32.00%	32.08%
OC9	20.59%	17.88%
OC10	45.38%	34.87%

II. Phase behavior

In order to analyze the target compounds for phase behavior, two different methods were applied. Initially, the target compounds were placed under a polarizing microscope and heated to desired temperatures followed by a return to room temperature. This allowed for the general assignment of phase transitions based on visual appearance. Nematic phases can be identified by the marbled, fluid and rainbow texture instead of what can be seen for crystalline (rigid and not marbled) or isotropic liquid (black and fully liquid).[1] There is a possibility that alternate liquid crystal phases could be seen such as the smectic phase but they can be differentiated from nematic if they appear to be more rigid and not marbled[1]. The microscope can also be used for determining fluidity as the slide can be pressed upon while it is cooling and the texture should shimmer if it is still fluid.

With this data collected, the samples were brought to a differential scanning calorimeter (DSC). Samples in this instrument were heated and cooled multiple times with exo- (pointed up) and endothermic peaks (pointed down) produced precisely at every phase transition. This allowed for an accurate determination of transition temperatures whose phase could be identified in conjunction with visual observations from the microscope. The size of the peaks represented the enthalpies of transition which were displayed next to the temperatures.

The OC5 target compound analysis produced promising results. With the microscope

runs, lower onset nematic temperatures were found compared to OC4 derivatives from previous research[10]. Further, the compound was found to stay relatively fluid all the way to around 34°C, also lower than what was seen previously. The visual appearance of this compound can be seen in Figure 6a and 6b which is consistant with what is expected from the nematic phase.

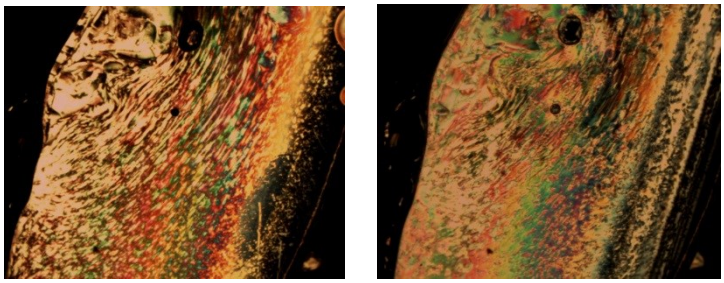

Figure 6a & b. OC5 nematic phase upon cooling at 72°C and 32°C respectively.

With the promising results of the microscope, this derivative was brought to the DSC for more precise analysis. The initial DSC heating (Figure 7a) showed that this compound first melted into a secondary crystalline phase at 71.13°C before going to the nematic phase at 82.69°C. It then went fully isotropic liquid at 129.10°C, and on cooling returned to nematic at 127.55°C remaining there until room temperature. Three more heats were performed and showed that it remained consistently in the nematic phase from room temperature until approximately 129°C where it cleared to the isotropic state (Figure 7b, see appendix).

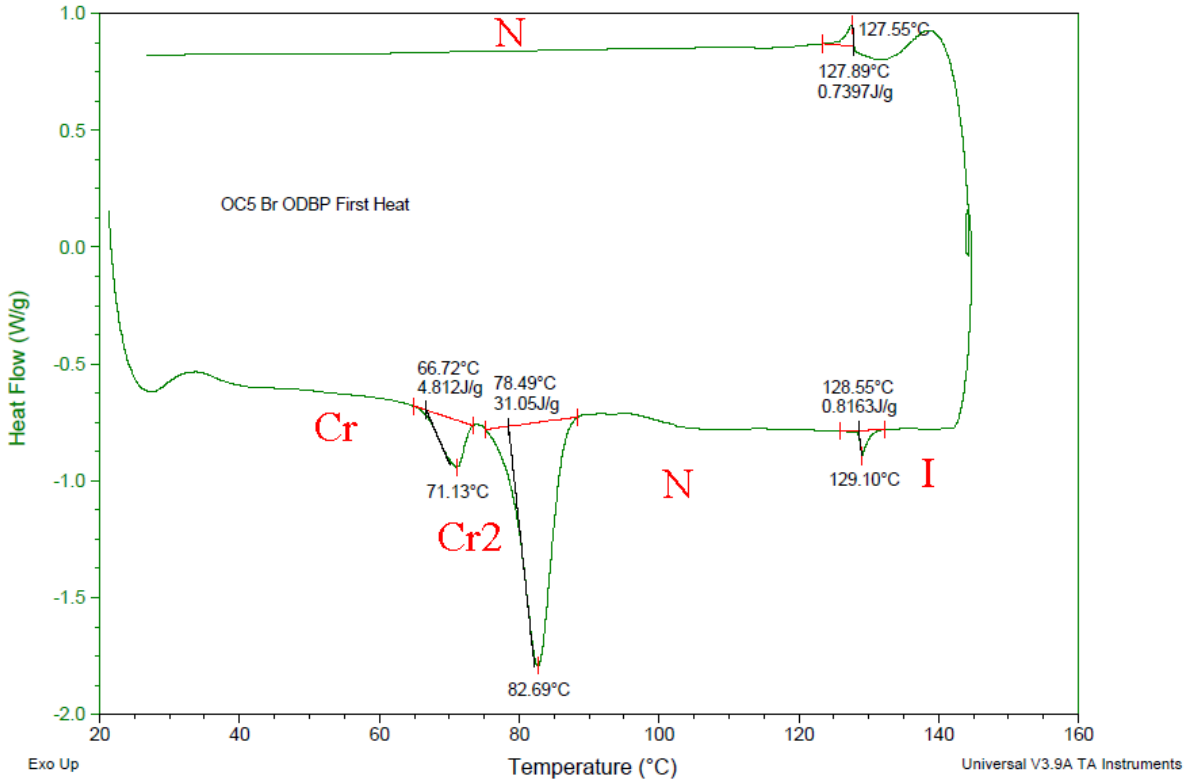

Figure 7a. DSC thermogram for OC5 initial heat.

The OC6 compound was fairly promising as well but with some odd variation. The microscope (Figures 8a and 8b) showed it to have some uncertainty in its initial melts. It appeared to go into a possible nematic phase around the mid 80°s but this may be a secondary crystalline phase. This appeared as a salmon-colored marbled texture until it reached ~120°C when the compound turned to a more fluid turquoise texture. This was followed by an interesting change in the mid 120°s where the color returned to a bright pink before going fully isotropic liquid at 130°C. Upon cooling it stayed nematic until room temperature; it remained fluid until about 35°C.

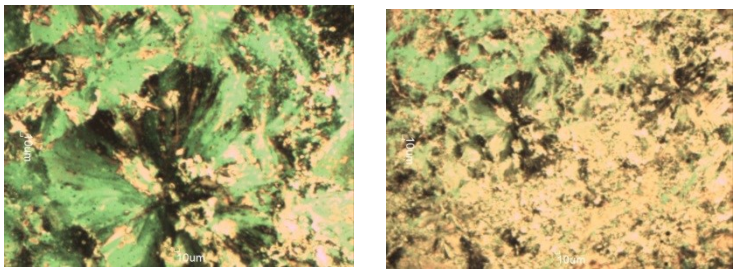

Figure 8a & b. OC6 nematic phase upon cooling at 75°C and 61°C respectively.

The initial DSC run (Figure 9a) helped explain what was seen under the microscope. At 83.76°C a fairly large endothermic peak showed a major transition. This transition is likely to a secondary crystalline phase because an even larger endothermic peak is seen at 113.24°C, more characteristic of that to a nematic transition. After that major transition it can be seen that there were two minor peaks where there should be just one. This could have something to do with the observations noticed under the microscope before it goes fully liquid at 130.26°C. The DSC then showed that upon cooling it stayed nematic from 128.68°C until room temperature. At this point the compound recrystallized to the secondary crystalline phase before being heated again. The next three heats showed more expected results with the compound transitioning from crystalline to nematic at 112.73°C and turning isotropic at 130.32°C (Figure 9c, appendix). To help understand what was occurring on the initial heat, the OC6 compound was rerun the following day to allow for overnight recrystallization. The DSC appeared very similar to the first heat except with only one endothermic peak after the nematic peak (Figure 9b).

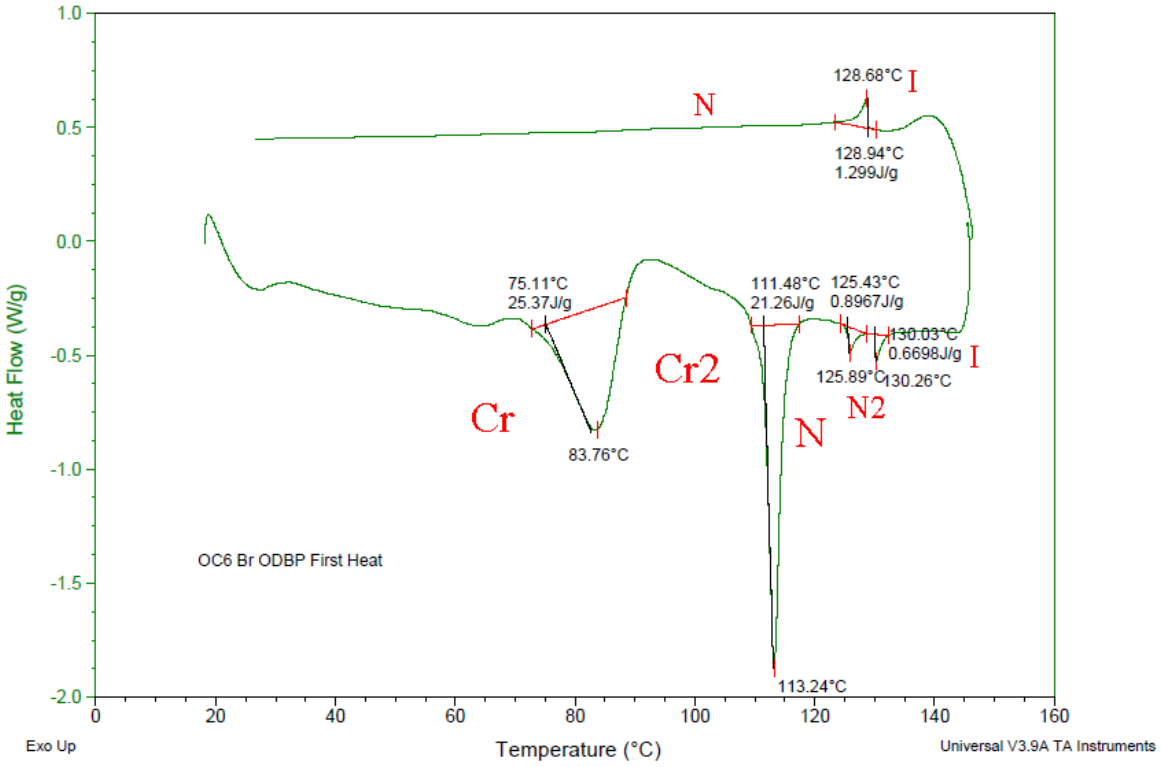

Figure 9a. DSC thermogram of OC6 on initial heat.

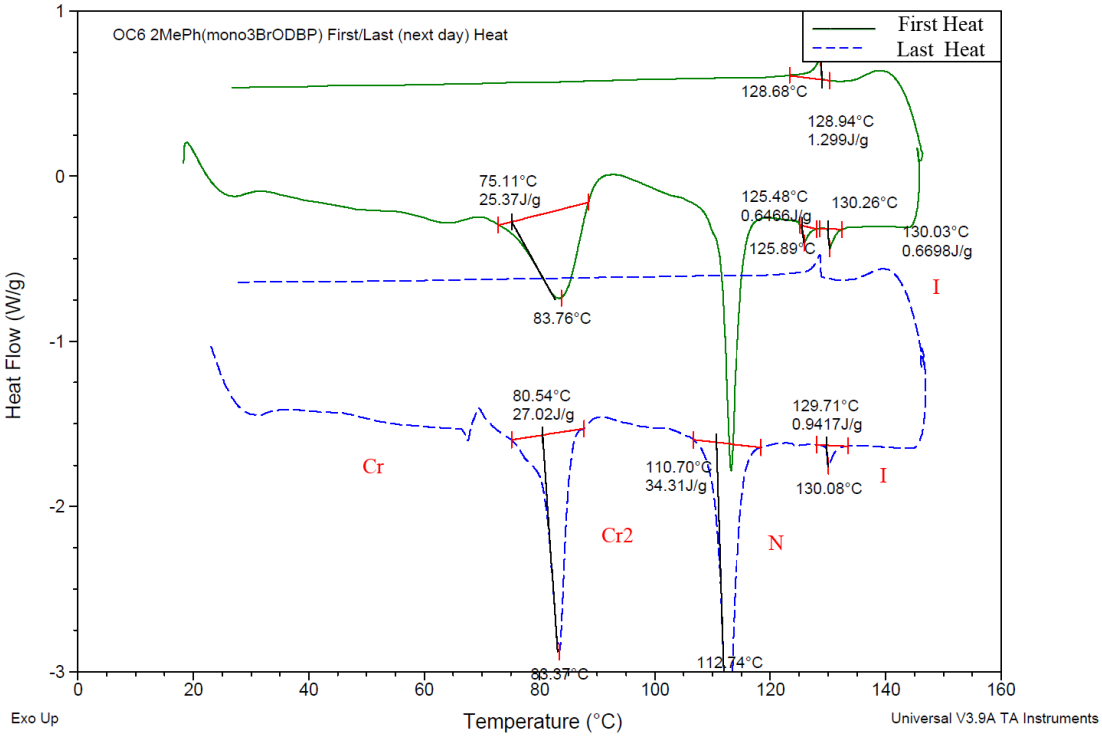

Figure 9b. DSC thermogram of OC6 first and last heats.

The OC7 target compound began to show a trend that was present in all of the longer chain compounds. The initial microscope run showed very little noticeable change until about 119.5°C when it went nematic. This nematic range, however, was very brief as it went fully isotropic at 122°C. Upon cooling it returned to nematic from isotropic at around 121°C and stayed nematic until room temperature. This compound proved to retain the best fluidity so far as it stayed quite liquid even into the mid-to-high 20°s. When it was reheated it began still in the nematic phase as opposed to the more thermodynamically stable crystalline phase. Once it was heated to about 50°C, enough energy was put into the system to allow it to overcome the energy barrier returning it to the secondary crystalline phase. This crystalline phase melted to the brief nematic phase at around the same 120°C temperature. These microscope images can be seen in Figure 10.

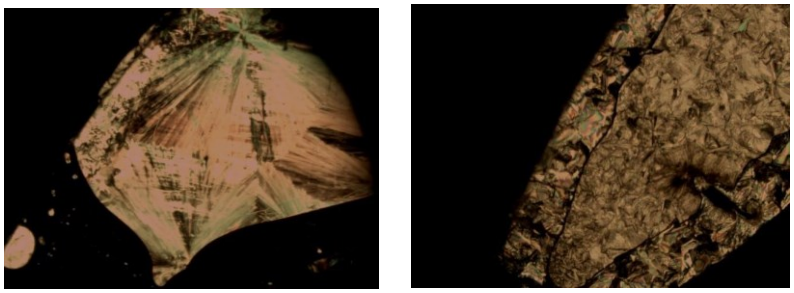

Figure 10a & b. OC7 cooling in nematic phase at 118°C and heating in the nematic phase at 29°C respectively

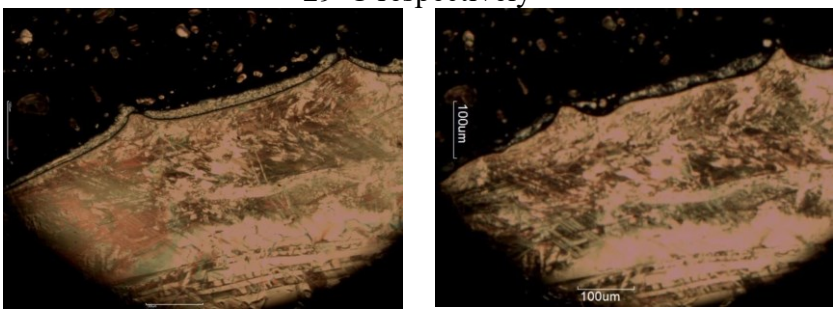

Figure 10c & d. OC7 in the nematic phase cooling at 26°C and cooling in the nematic phase at 40°C respectively.

The DSC reveals that in the initial heat (Figure 11a) there was a small but broad transition peak from the primary crystalline phase to the secondary at 76.39°C. Then at 120.34°C

a very large endothermic peak was seen and no others are found beyond it. This is because the nematic and isotropic peaks show up as one due to the brief nematic range. Upon cooling the compound was returned to nematic at 121.02°C. The subsequent runs showed the exothermic peak at 50°C as the compound returned from nematic to crystalline. This was followed by an endothermic peak signifying the crystalline melted into another crystalline phase. This phase was returned to nematic and then isotropic at 120.51°C. An overlay of the first and second runs is shown in Figure 11b.

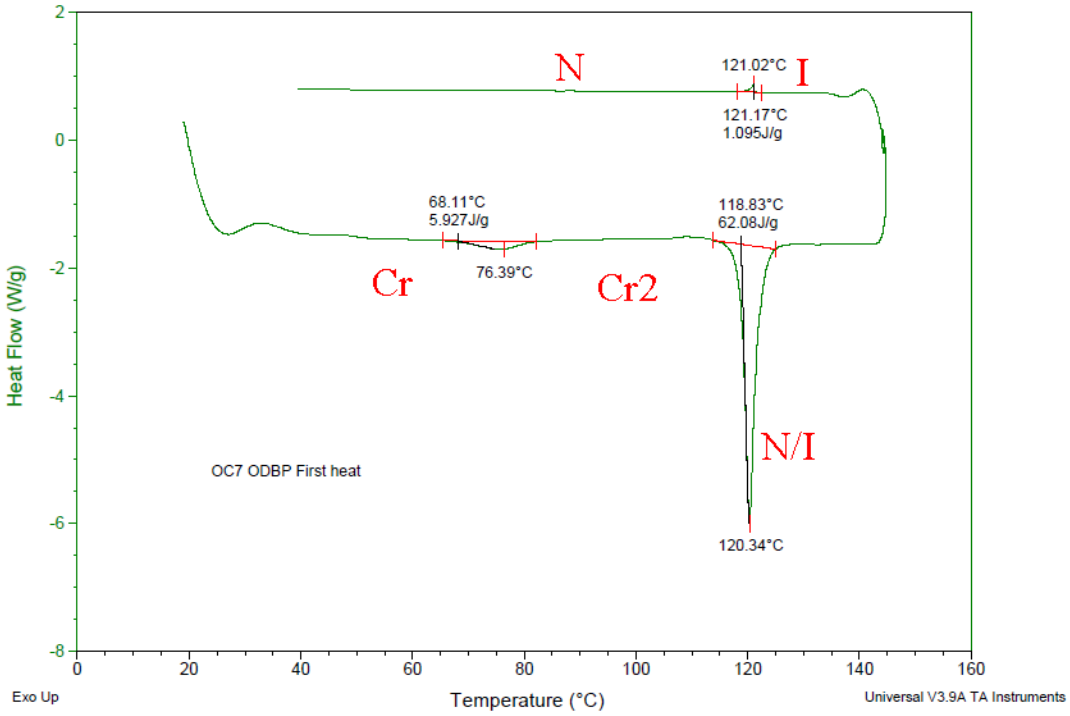

Figure 11a. DSC thermogram of OC7 target compound on initial heating.

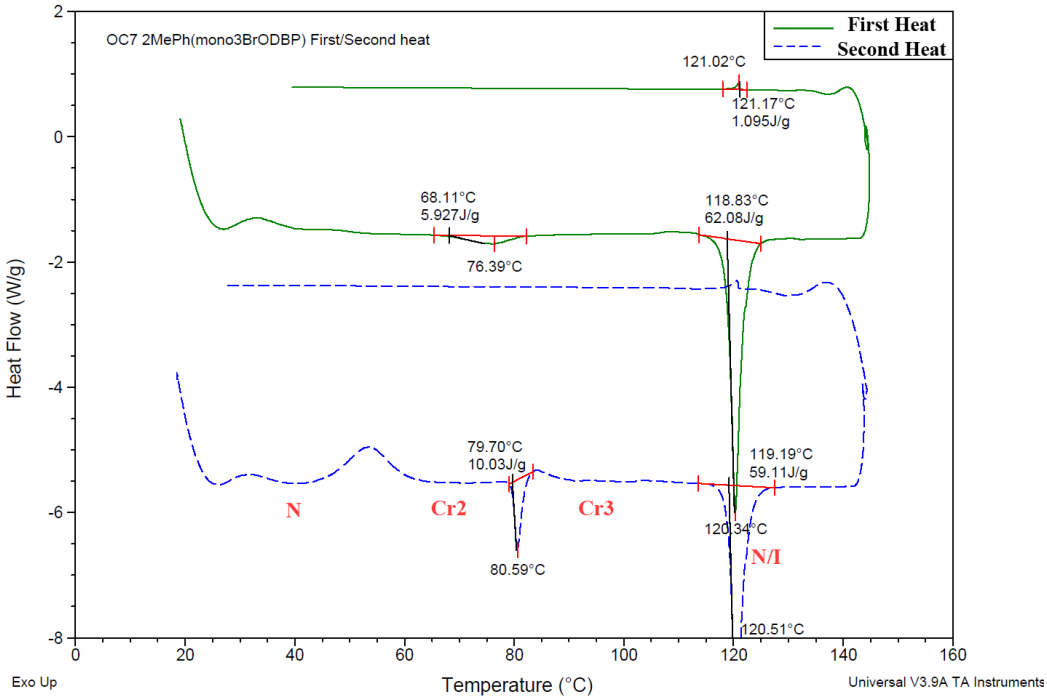

Figure 11b. DSC thermogram of OC7 target compound first and second heatings.

The first microscope run for the OC8 target compound showed its initial signs of melting at 114°C where it went straight into the nematic phase without any secondary crystalline phase. This nematic phase only lasted a few degrees as it quickly went was isotropic at about 120°C. This range was very small, similar to that of the OC7. Upon cooling it stayed in the nematic phase until room temperature and also remained very fluid all the way down to 34°C, and still semi-fluid at 27°C. Because of this, the later runs started in the nematic phase and transitioned to secondary crystalline once the energy barrier was able to be surmounted. The microscope pictures can be seen in Figure 12.

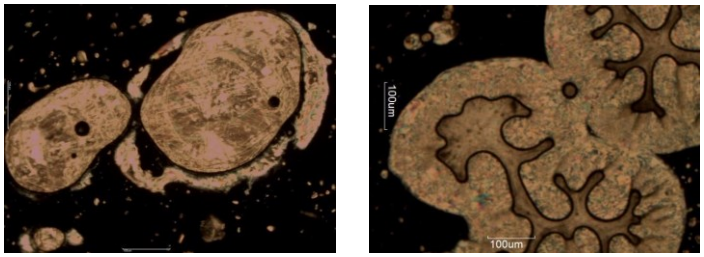

Figure 12. OC8 cooling in the nematic phase at 50°C and 34°C respectively.

When looking at the DSC (Figure 13a) it can be seen that no secondary crystalline phase was observed in the initial heating of the OC8 compound. It remained crystalline until 116.48°C at which point the very brief nematic phase occurred. This was represented by one very large peak similar to the one seen for the OC7. After this peak the compound was in the isotropic liquid phase. Upon cooling the compound returned to nematic at 117.74°C and stayed there until room temperature. The later run DSCs showed the exothermic peak as the cool nematic phase returned to secondary crystalline between 40-65°C (Figure 13b, appendix).

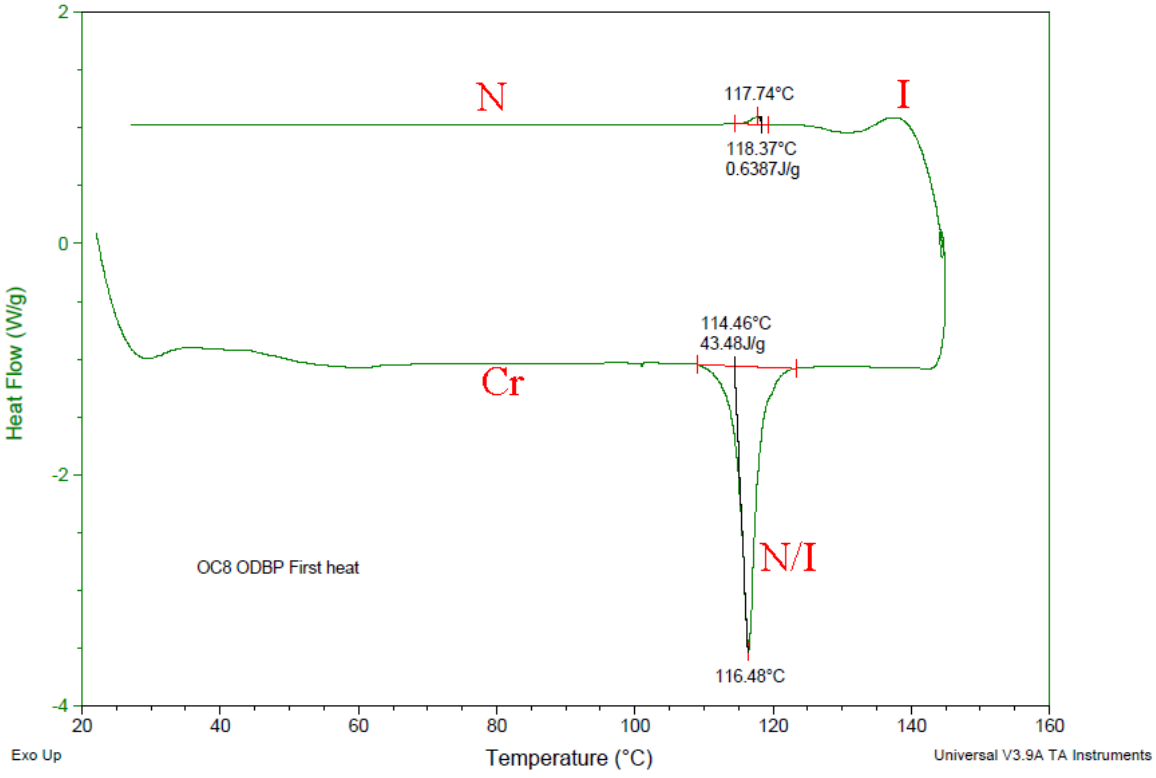

Figure 13a. DSC thermogram of OC8 target compound initial heating.

Under microscopic analysis, the OC9 target compound (Figure 14) showed its first signs of melting around 106-109°C but then appeared to go fully isotropic at about 115°C, displaying a slightly larger but again brief nematic phase. When it cooled it stayed in nematic all the way to low temperatures but had difficulty retaining its fluidity as it started to recrystallize by about 39°C**.** When reheated, it began in a brown crystalline phase (see left figure below) and did not return to nematic until about 100°C followed by isotropic at 116°C.

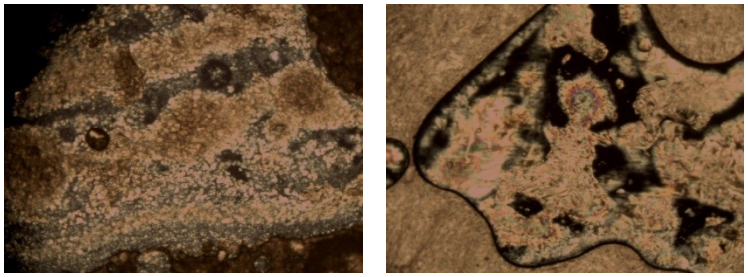

Figure 14. OC9 target compound in secondary crystalline phase heating at 68°C and cooling in nematic phase at 50°C respectively.

The initial DSC (Figure 15a) showed that there appeared to be a melting to the secondary crystalline phase at 95.39°C followed by the nematic transition at 106.55°C. It remained nematic until 114.63°C where it went isotropic. Upon cooling it returned to the nematic phase at 113.10°C and stayed there until the high 30°s. However, it recrystallized prior to room temp and the subsequent heats began in the secondary crystalline phase. According to the DSC (Figure 15b), there appeared to be multiple transitions from that crystalline phase to other crystalline phases at 87.26°C and 95.69°C before making it all the way to nematic at 106.55°C.

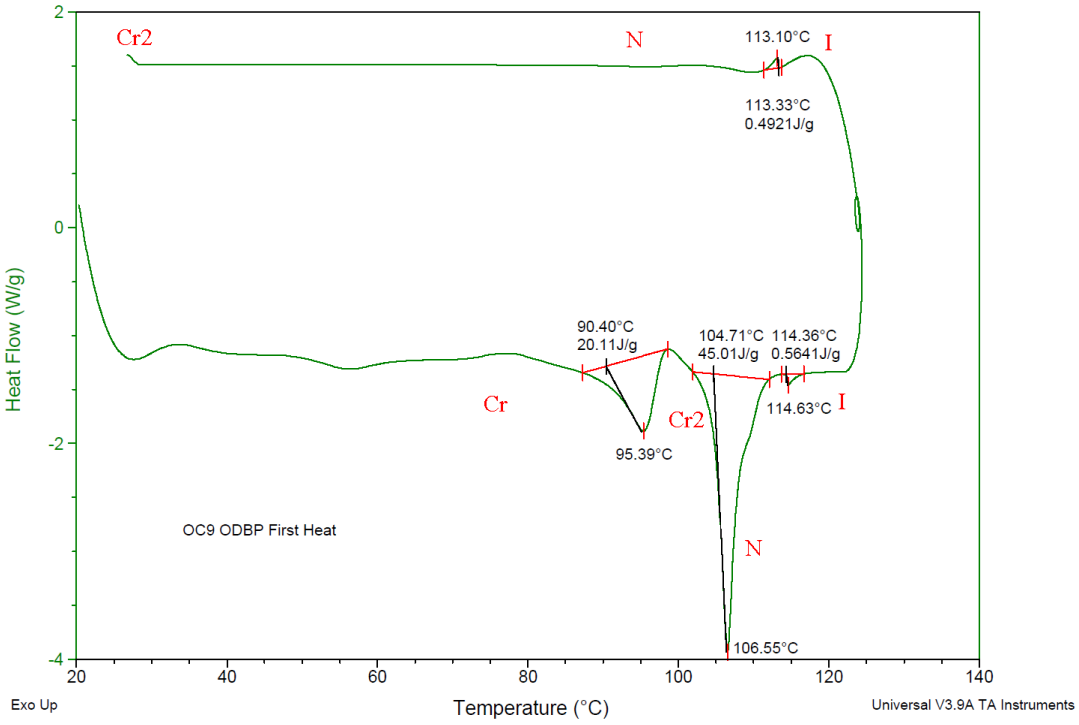

Figure 15a. DSC thermogram of OC9 target compound on initial heating.

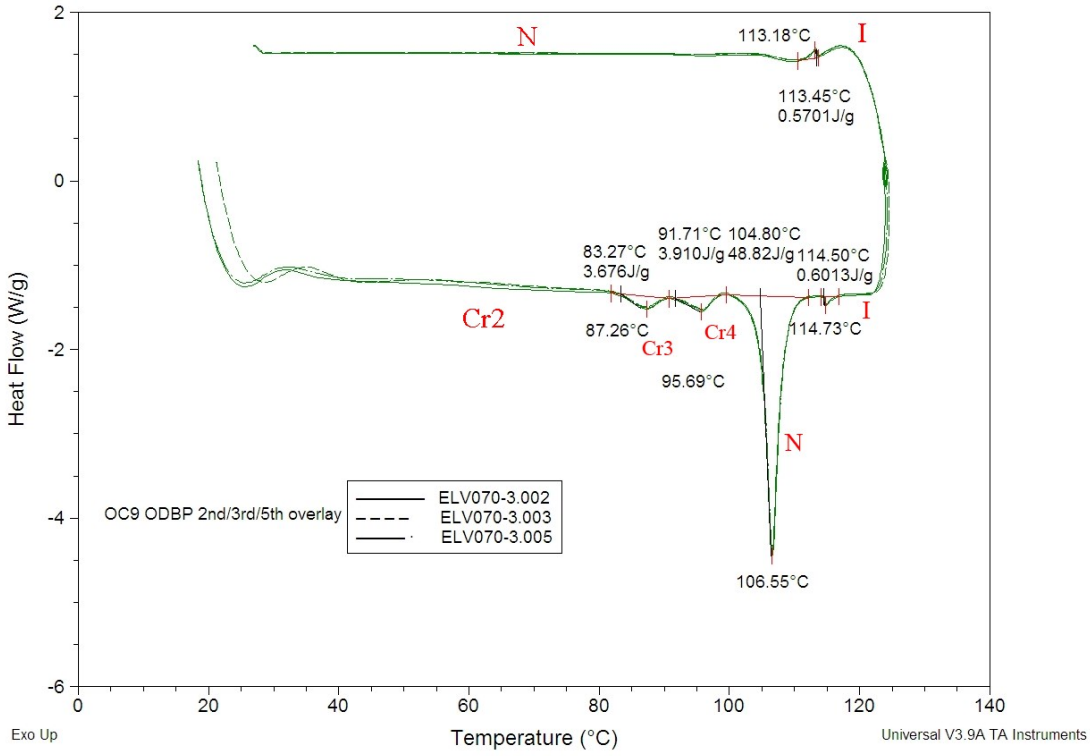

Figure 15b. DSC thermogram of OC9 target compound subsequent heatings.

The final target compound, OC10 did not appear to melt until around 119°C when viewed under the microscope (Figure 16). It went almost immediately to isotropic liquid at around 122°C. When it cooled it returned to the nematic phase at 110.5°C but at temperatures below 40°C it started to return to a secondary crystalline phase, similar to the OC9 compound. In the subsequent heats the compound appeared to remain in the secondary crystalline phase with some partial melting around 100°C but not going fully nematic at about 118-120°C.

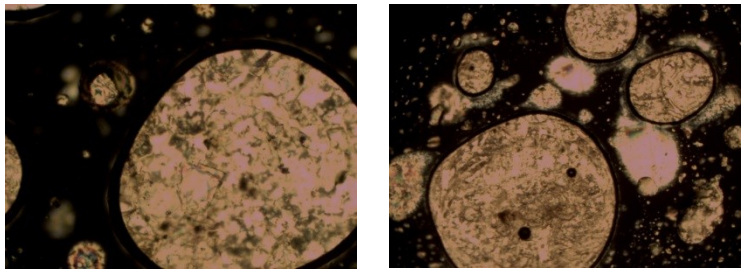

Figure 16. OC10 in the nematic phase cooling at 112°C and 67°C respectively.

As seen on the DSC, the initial heat (Figure 17a) revealed that there was a minor exothermic peak at 71.27°C signifying that this compound could be crystallizing to another state with heat applied. There were no other peaks until the extremely large endothermic peak at 119.09°C which contained the nematic and isotropic transitions. Upon cooling, the compound returned to nematic at 112.28°C but then at 45.37°C a distinct peak was seen for its recrystallization. Knowing that this compound began in a crystalline phase, the following heats (Figure 17b) showed an exothermic peak at 86.76°C before reaching the nematic/isotropic peak at 119.11°C. This means that it is recrystallizing to a more thermodynamically stable crystalline form, an odd characteristic to see for a compound that was already crystalline before heat was applied.

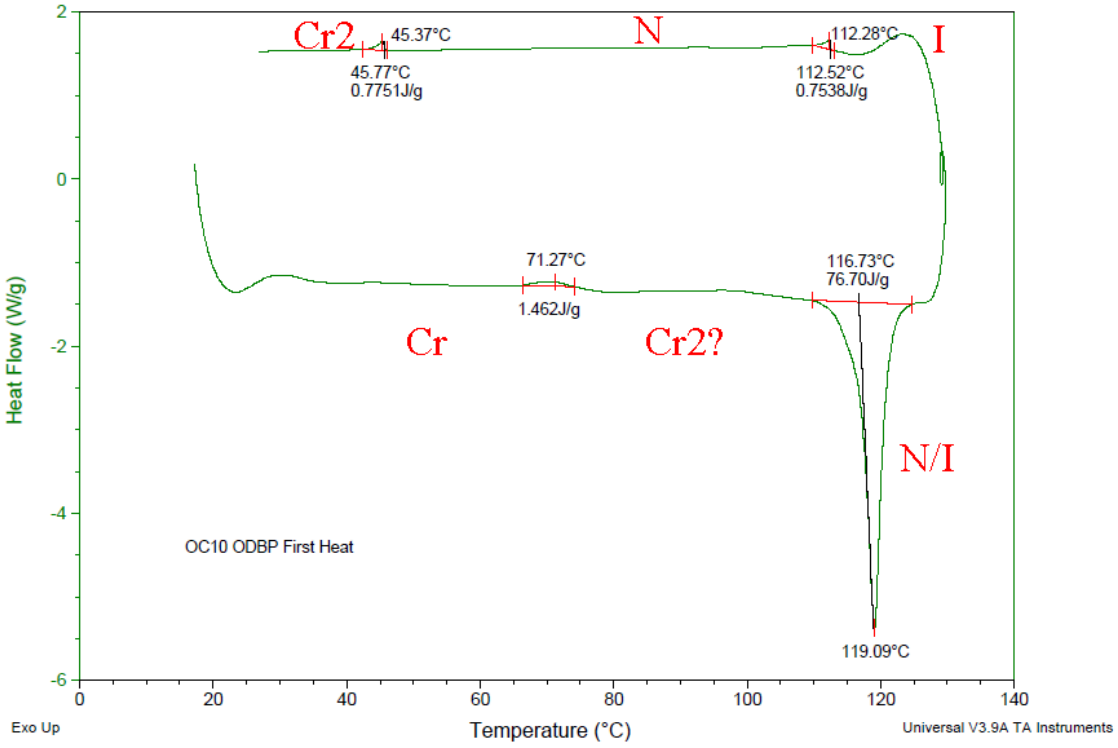

Figure 17a. DSC thermogram of OC10 target compound on initial heating.

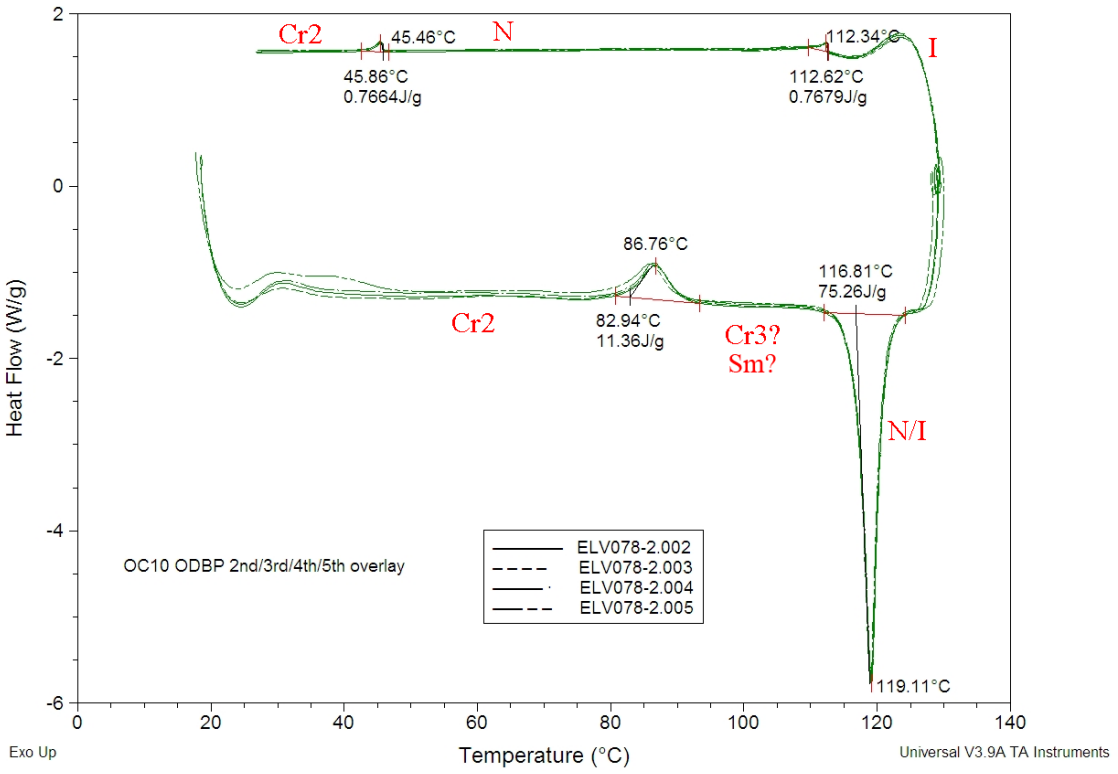

Figure 17b. DSC thermogram of OC10 target compound subsequent heats.

As summarized in Table 2 and Figure 18, the nematic phase generally occurs at lower temperatures for the shorter terminal alkyl chain lengths. This phase also has a larger range for the shorter derivatives. Even though the OC7 and OC8 had very brief nematic ranges at higher temperatures, they retained the most fluidity at lower temperatures than the others. The longest length chains of 9 and 10 exhibited strange characteristics coming from their secondary crystalline phases, maybe there is the presence of a smetic phase between crystalline and the brief nematic ones seen. There is a bit of discrepancy with the OC9 between microscope and DSC as there were numerable endothermic transitions that were not noticed under the microscope. Further, the strange OC10 exothermic peaks are very curious leading one to believe that it may be crystallizing from a softer crystalline phase to a more stable one with heat.

Table 2. Transition temperatures and enthalpies on initial heating.

Compound	**Phase transition temperature (°C) and enthalpy (kJ/mol)**
OC5 2MePh(mono3BrODBP)	Cr 71.13 (3.72) Cr2 82.69 (24.0) N 129.1 (0.63) I
OC6 2MePh(mono3BrODBP)	Cr 83.76 (20.33) Cr2 113.2 (17.04) N 125.9 (0.72) N2 130.3 (0.54) I
OC7 2MePh(mono3BrODBP)	Cr 76.39 (4.9) Cr2 119.5[a] (51.5)[b] N 122[a] (51.5)[b] I
OC8 2MePh(mono3BrODBP)	Cr 114[a] (37.3)[b] N 120[a] (37.3)[b] I
OC9 2MePh(mono3BrODBP)	Cr 95.39 (17.8) Cr2 106.5 (39.9) N 114.6 (0.5) I
OC10 2MePh(mono3BrODBP)	Cr 71.27 (1.33) Cr2 119[a] (70.1)[b] N 122[a] (70.1)[b] I

a = polarizing microscope temperatures; b = combined enthalpies

Figure 18 shows a comparison of all six compounds, their first two heats, and their cooling using initial heating temperatures from Table 2. This allows for easy viewing of trends between the compounds.

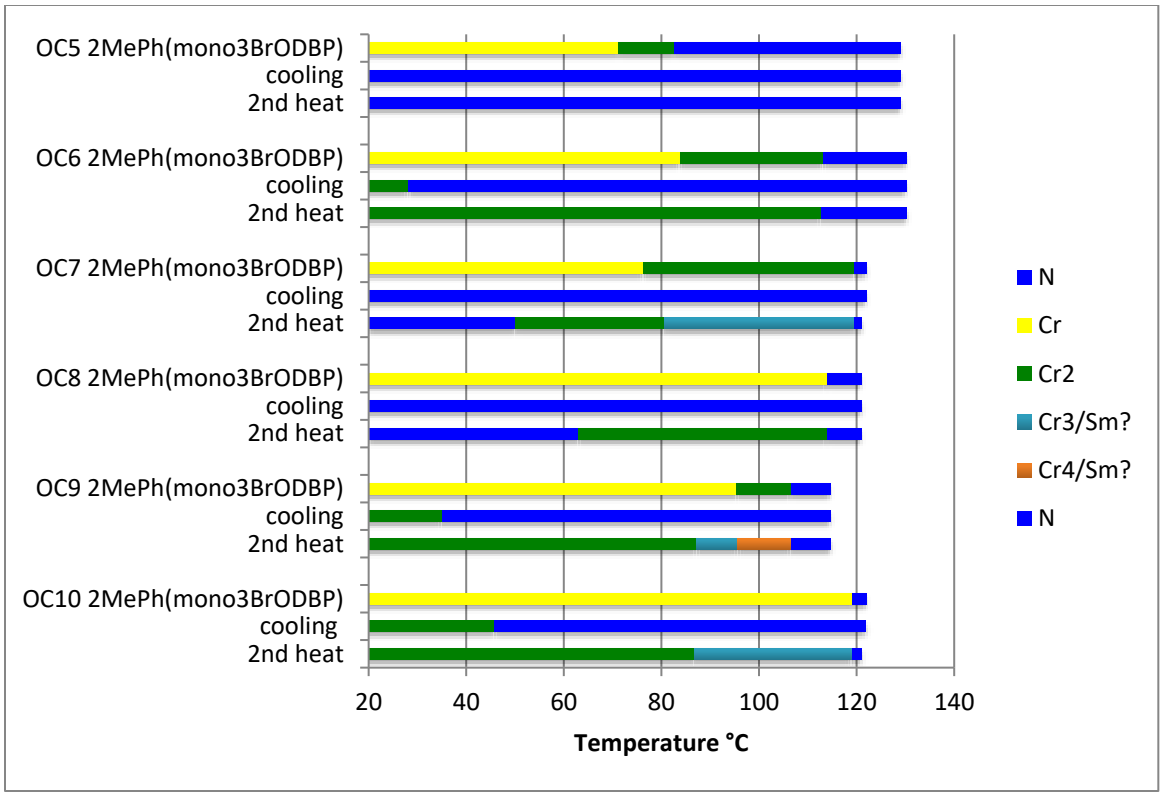

Figure 18. Phase behavior graph of six target compounds in their first two heats and a cooling.

Experimental

4-Hydroxy-3-bromo-*N*-(4-hydroxybenzoyl) benzhydrazide. 3-bromo-4-hydroxybenzoic acid (2.0101 g, 9.26 mmol), 4-hydroxybenzhydrazide (1.4467 g, 9.51 mmol), and 1-hydroxybenzotriazole hydrate (HOBt) (1.2777 g, 9.46 mmol), were added to a 100 mL round bottom flask followed by dimethylformamide (DMF) (40 mL) and this mix was stirred. Ethyl dimethylaminopropyl carbodiimide hydrochloride (EDC) (1.8202 g, 9.50 mmol) was added to the solution and rinsed in with DMF (3 mL). After stirring for two days under nitrogen, the product was slowly pipetted into DI water (200 mL) while stirring in a round bottom flask. A cloudy white precipitate formed immediately. This solution was left stirring for 30 min. The white precipitate was collected by Büchner filtration and washed three times with DI water. It was then dried via vacuum oven for two hours. Recrystallization was performed with pure ethanol (20 mL) in an Erlenmeyer flask. At first, the product refused to go into solution, more ethanol (20 mL) was added as the mixture was boiling. After an hour of stirring, the solution still remained cloudy, acetone was added (2x10 mL) and left to settle for a few more hours. The precipitate was collected via Büchner filter and washed with 2:1 ethanol/acetone. An ^{1}H-NMR was taken with DMSO, but the product appeared to have starting material. It was dissolved in 5% $NaHCO_3$ (20 mL) to remove any benzoic acid, filtered via Büchner, and washed with DI water. This was repeated with 5% HCl to remove any hydrazide. Final product yielded a yellow-

white flaky powder **2** (2.122 g, 65.2%). ^{1}H-NMR (400 MHz, DMSO-d_6) δ 6.81 (d, 2H, J = 8.8 Hz), 7.00 (d, 1H, J = 8.4 Hz), 7.76 (d, 3H, J = 8.8 Hz), 8.06 (s, 1H), 10.16 (s, 2H), 10.25 (s, 2H).

2-(4-Hydroxy-3-bromophenyl)-5-(4-hydroxyphenyl)-1,3,4-oxadiazole. 4-Hydroxy-3-bromo-*N*-(4-hydroxybenzoyl) benzhydrazide (0.438 g, 1.25 mmol) and thionyl chloride (1.809 mL, 24.9 mmol) were added to a 50 mL round bottom flask equipped with a reflux condenser and a gas trap. The solution was left to reflux for 4 hours and then allowed to cool to room temperature. It was then poured over approximately 50 mL of ice in a beaker and covered with a watch glass. The solution hissed and popped as a yellow/red precipitate formed. It was allowed to stir for an hour as the ice melted. The product was stirred and collected via Büchner filtration and washed with DI water. The crude yellow powder was dissolved in a solution of ethanol (15 mL) and DI water (15 mL) as it was recrystallized. The yellow precipitate was collected via Büchner and washed with the ethanol/DI solution, followed by a vacuum oven to dry yielding product **3** (0.2443 g, 58.8%): ^{1}H-NMR (400 MHz, DMSO-d_6) δ 6.92 (d, 2H, J = 8.8 Hz), 7.10 (d, 1H, J = 8.8 Hz), 7.89-7.93 (m, 3H, J = 8.8 Hz), 8.15 (d, 1H, J = 2.4 Hz), 10.29 (s, 1H).

Ethyl 4-hydroxy-2-methyl benzoate. 4-hydroxy-2-methylbenzoic acid (3.0028 g, 19.7 mmol) was dissolved in absolute ethanol (40 mL) in a round bottom flask to form a clear-yellow liquid. Concentrated sulfuric acid (1 mL, 18.7 mmol) was pipetted into the mix. A reflux condenser was attached and the solution was refluxed overnight. Some of the ethanol was removed by rotary evaporation to make the solution more concentrated for the workup. Ethyl ether (50 mL) was added to the solution and this was transferred to a separatory funnel. The organic layer was washed twice with DI water and once with 5% $NaHCO_3$ followed by a back extraction of the aqueous washings with fresh ether. The combined organic extracts were dried with $MgSO_4$, filtered, and solvent removed to form a white powder. An ^{1}H-NMR spectrum was taken of the product with deuterated acetone and it appeared to still have starting material. The product was dissolved in ethyl ether (40 mL) and washed in a separatory funnel twice with 5% $NaHCO_3$ and once with DI water (20 mL). The Ether layer was dried with $MgSO_4$, filtered, and rotary evaporated to produce a white powder (2.337 g, 65.7%). ^{1}H-NMR (400 MHz, Acetone-d_6) δ 1.29 (t, 3H, J = 7.0 Hz), 2.48 (s, 3H), 4.20-4.25 (m, 2H), 6.69-6.71 (m, 2H), 7.79-7.81 (m, 1H).

Ethyl 4-pentoxy-2-methyl benzoate. Ethyl 4-hydroxy-2-methyl benzoate (0.3116 g, 1.73 mmol) was dissolved in DMF (8.4 mL) in a 100 mL round bottom flask. Cesium carbonate (0.8182 g, 2.51 mmol) was added under nitrogen. 1-bromopentane (0.3860 g, 2.56 mmol) was added dropwise to the stirring slurry under nitrogen. This reaction was left stirring under nitrogen overnight. Reaction completion was checked with TLC (eluent 1:1 hexanes-ether, R_f = 0.78) before being worked up. DI water (20 mL) was added to the solution and this was transferred to a separatory funnel. At this point DI water (20 mL) was added again followed by ether (25 mL). The organic layer was washed two more times with DI water, followed by a back extraction of the combined aqueous layer with fresh ether. The combined organic layers were dried with $MgSO_4$, filtered, and solvent removed by rotary evaporation to produce an oily substance (0.2466 g, 56.99%). ^{1}H-NMR (400 MHz, $CDCl_3$) δ 0.92 (t, 3H, J = 7.2 Hz), 1.34-1.45 (m, 7H), 1.74-1.82 (pentet, 2H, J = 7.0 Hz), 2.58 (s, 3H), 3.98 (t, 2H, J = 6.6 Hz), 4.28-4.33 (q, 2H, J = 7.2 Hz), 6.70-6.72 (m, 2H), 7.91 (d, 1H, 9.6 Hz).

4-pentoxy-2-methyl benzoic acid. Ethanol (25 mL) was added to ethyl 4-pentoxy-2-methyl benzoate (0.2466 g, 0.986 mmol) in the same 100 mL round bottom flask. Potassium hydroxide

(0.2889 g, 5.15 mmol) was dissolved in minimal DI water and added to the solution. A reflux condenser and heating mantle were attached to allow the reaction to reflux for 4.5 hours with stirring. Ethanol was removed by rotary evaporation. DI water (30 mL) was added and then the solution was made acidic by adding 6M HCl. The solution was left sitting overnight and a precipitate formed. The white flaky precipitate was collected via Büchner filtration and washed with DI water. The product was then recrystallized with ethanol (10 mL) and DI water (~15 mL), collected via Büchner, and washed with 1:1 ethanol/DI mix leaving a shiny white powder (0.1256 g, 57.35%). ^{1}H-NMR (400 MHz, $CDCl_3$) δ 0.93 (t, 3H, J = 7.2 Hz), 1.37-1.48 (m, 4H), 1.76-1.83 (pentet, 2H, J = 7.0 Hz), 2.62 (s, 3H), 3.99 (t, 2H, J = 6.6 Hz), 6.74-6.76 (m, 2H), 8.02 (d, 1H, J = 4.8 Hz).

Ethyl 4-hexyloxy-2-methyl benzoate. A procedure identical to that used for ethyl 4-pentoxy-2-methyl benzoate was utilized except with ethyl 4-hydroxy-2-methyl benzoate (0.4014 g, 2.23 mmol), cesium carbonate (1.0948 g, 3.36 mmol), 1-iodohexane (0.7056 g, 3.33 mmol), and DMF (11.1 mL). The product was checked for completion by TLC (eluent 1:1 hexanes-ether, R_f = 0.63) to yield an oily liquid (0.3690 g, 62.7%). ^{1}H-NMR (400 MHz, $CDCl_3$) δ 0.90 (t, 3H, J = 5.0 Hz), 1.26-1.38 (m, 7H), 1.41-1.48 (pentet, 2H, J = 7.4 Hz), 1.74-1.81 (pentet, 2H, J = 7.4 Hz), 2.58 (s, 3H), 3.98 (t, 2H, J = 6.6 Hz), 4.28-4.33 (q, 2H, J = 7.2 Hz), 6.70-6.73 (m, 2H), 7.91 (d, 1H, J = 9.6 Hz).

4-hexyloxy-2-methyl benzoic acid. Ethanol (5 mL) was added to ethyl 4-hexyloxy-2-methyl benzoate in the previously used round bottom flask and transferred to 35 mL microwave vial. Ethanol (5 mL) was added to the round bottom to rinse any remaining product and this was transferred to the microwave vial. Potassium hydroxide (0.3323 g, 5.92 mmol) was dissolved in minimal DI water and pipetted into the microwave vial. The solution was stirred before being placed in the microwave which heated it to 140°C for 7 minutes. After the microwave run was complete, the solution was transferred to an erlenmeyer flask and DI water (30 mL) was added. It was then acidified with 6M HCl and stirred for 10 min. The white powder precipitate was collected via Büchner filtration. The crude product was recrystallized from ethanol (10 mL) followed by DI water (15 mL). The white precipitate was collected by Büchner and washed with 1:1.5 ethanol/water mix (0.1798 g, 54.5%). ^{1}H-NMR (400 MHz, $CDCl_3$) δ 0.90 (t, 3H, J = 5.6 Hz), 1.34 (m, 4H), 1.46 (pentet, 2H, J = 6.8 Hz), 1.80 (pentet, 2H, J = 7.0 Hz), 2.62 (s, 3H), 3.99 (t, 2H, J = 6.4 Hz), 6.74 (m, 2H), 8.03 (d, 1H, J = 8.4 Hz).

Ethyl 4-heptyloxy-2-methyl benzoate. An identical procedure to ethyl 4-pentoxy-2-methyl benzoate was used except with 4-hydroxy-2-methyl ethyl benzoate (0.4017 g, 2.23 mmol), cesium carbonate (1.0927 g, 3.35 mmol), 1-iodoheptane (0.7618 g, 3.37 mmol), and DMF (11.1 mL). This reaction was checked for completion by TLC (eluent 1:1 hexanes-ether, R_f = 0.81); workup yielded an oily liquid (0.1876 g, 30.25%). ^{1}H-NMR (400 MHz, $CDCl_3$) δ 0.88 (t, 3H, J = 6.8 Hz), 1.28-1.38 (m, 9H), 1.40-1.48 (pentet, 2H, J = 6.9 Hz), 1.74-1.81 (pentet, 2H, J = 7.6 Hz), 2.582 (s, 3H), 3.96-3.99 (t, 2H, J = 6.6 Hz), 4.28-4.33 (q, 2H, J = 7.2 Hz), 6.70-6.72 (m, 2H), 7.91 (d, 1H, J = 9.2 Hz).

4-heptyloxy-2-methyl benzoic acid. Potassium hydroxide (1.7355 g, 30.89 mmol) dissolved in minimal DI water and ethanol (15 mL) were added to 4-heptoxy-2-methyl ethyl benzoate in the previously used round bottom flask to avoid product loss. The solution was capped and left stirring overnight at room temperature. It was then concentrated by removing ethanol with rotary

evaporation. Approximately 40 mL of DI water were added to the solution and it was acidified using 6M HCl. The white precipitate was filtered out via Büchner and washed with a DI water wash. The product was recrystallized using ethanol (15 mL) and DI water (20 mL) to give a white powder (0.1251 g, 74.15%). ^{1}H-NMR (400 MHz, $CDCl_3$) δ 0.88 (t, 3H, J = 6.2 Hz), 1.27-1.38 (m, 6H), 1.41-1.47 (pentet, 2H, J = 7.6 Hz), 1.75-1.82 (pentet, 2H, J = 6.9 Hz), 2.62 (s, 3H), 3.99 (t, 2H, J = 6.6 Hz), 6.74 (m, 2H), 8.02 (d, 1H, J = 9.2 Hz).

4-Octyloxy-2-methyl benzoic acid. Ethyl 4-hydroxy-2-methyl benzoate (0.4035 g, 2.24 mmol) was dissolved in DMF (11.1 mL) in a 100 mL round bottom flask. Cesium carbonate (1.0859 g, 3.33 mmol) was added under nitrogen, forming a precipitate followed by 1-iodooctane (0.8055 g, 3.35 mmol) which was added dropwise to the stirring solution. The reaction was left stirring overnight still under nitrogen. The product was worked up by mixing DI water (20 mL) with the solution. It was then transferred to a separatory funnel where DI water (20 mL) and ether (25 mL) were added. The organic layer was washed two more times with DI water, followed by a back extraction of the aqueous washings with fresh ether. The combined ether extracts were dried with $MgSO_4$, filtered, and concentrated by rotary evaporated to produce an oily substance. Potassium hydroxide (1.7429 g, 31.06 mmol) dissolved in minimal DI water and ethanol (15 mL) were added to the oily product in the round bottom flask. The solution was then capped and left stirring overnight at room temperature. It was then concentrated by removing ethanol using rotary evaporation. Approximately 40 mL of DI water were added to the solution and it was acidified using 6M HCl. The white precipitate was filtered out via Büchner and washed with DI water. At first the crude product was not fully hydrolyzed from examining the ^{1}H-NMR spectrum so it was refluxed with ethanol (15 mL) and KOH (0.3065 g, 5.46 mmol) for approximately three hours. This was acidified and collected as described previously. It was recrystallized using ethanol (20 mL) and DI water (10 mL) to yield a white powder (0.1898 g, 32.08%). ^{1}H-NMR (400 MHz, $CDCl_3$) δ 0.86-0.90 (t, 3H, J = 6.8 Hz), 1.28-1.36 (m, 8H), 1.41-1.49 (pentet, 2H, J = 7.2 Hz), 1.75-1.82 (pentet, 2H, J = 7.1 Hz), 2.62 (s, 3H), 3.99 (t, 2H, J = 6.6 Hz), 6.74-6.76 (m, 2H), 8.04 (d, 1H, J = 9.6 Hz).

Ethyl 4-nonyloxy-2-methyl benzoate. A procedure identical to ethyl 4-pentoxy-2-methyl benzoate was used except with ethyl 4-hydroxy-2-methyl benzoate (0.4003 g, 2.22 mmol), cesium carbonate (1.0939 g, 3.35 mmol), 1-iodononane (0.8488 g, 3.34 mmol), and DMF (11.1 mL). Product checked for completion by TLC (eluent 1:1 hexanes-ether, R_f = 0.55) to yield an oily liquid (0.6232 g, 91.56%). ^{1}H-NMR (400 MHz, $CDCl_3$) δ 0.88 (t, 3H, J = 6.6 Hz), 1.27-1.38 (m, 13H), 1.40-1.47 (pentet, 2H, J = 7.2 Hz), 1.74-1.82 (pentet, 2H, J = 7.7 Hz), 2.58 (s, 3H), 3.98 (t, 2H, 6.6 Hz), 4.28-4.33 (q, 2H, J = 7.2 Hz), 6.70-6.72 (m, 2H), 7.91 (d, 1H, J = 9.6 Hz).

4-Nonyloxy-2-methyl benzoic acid. The procedure and recrystallization are identical to that for 4-heptoxy-2-methyl benzoic acid except with ethyl 4-nonyloxy-2-methyl benzoate (0.6232 g, 2.03 mmol) and KOH (1.7065 g, 30.41 mmol). This yielded a flaky white powder (0.1211 g, 21.39%). ^{1}H-NMR (400 MHz, $CDCl_3$) δ 0.88 (t, 3H, J = 6 Hz), 1.20-1.34 (m, 10H), 1.41-1.46 (pentet, 2H, J = 6.9 Hz), 1.75-1.81 (pentet, 2H, J = 6.6 Hz), 2.62 (s, 3H), 3.99 (t, 2H, J = 5.9 Hz), 6.74-6.76 (m, 2H), 8.03 (d, 1H, J = 9.2 Hz).

Ethyl 4-decyloxy-2-methyl benzoate. A procedure identical to ethyl 4-pentoxy-2-methyl benzoate was used except with ethyl 4-hydroxy-2-methyl benzoate (0.3089 g, 1.71 mmol),

cesium carbonate (0.8411 g, 2.57 mmol), 1-iododecane (0.6990 g, 2.57 mmol), and DMF (8.57 mL). Product checked for completion by TLC (eluent 1:1 hexanes-ether, $R_f = 0.67$) to yield an oily liquid (0.2872 g, 52.3%). ^{1}H-NMR (400 MHz, $CDCl_3$) δ 0.87 (t, 3H, $J = 6.6$ Hz), 1.26-1.38 (m, 15H), 1.40-1.47 (pentet, 2H, $J = 7.1$ Hz), 1.73-1.81 (pentet, 2H, $J = 7.5$ Hz), 2.58 (s, 3H), 3.97 (t, 2H, $J = 6.6$ Hz), 4.28-4.33 (q, 2H, $J = 7.0$ Hz), 6.70-6.72 (m, 2H), 7.91 (d, 1H, $J = 9.6$ Hz).

4-Decyloxy-2-methyl benzoic acid. The procedure and recrystallization are identical to 4-heptoxy-2-methyl benzoic acid except with ethyl 4-decyloxy-2-methyl benzoate (0.2872 g, 0.897 mmol) and KOH (1.8002 g, 32.08 mmol). This yielded a flaky white powder (0.1747 g, 34.87%). ^{1}H-NMR (400 MHz, $CDCl_3$) δ 0.88 (t, 3H, $J = 6.8$ Hz), 1.26-1.39 (m, 12H), 1.41-1.48 (pentet, 2H, $J = 7.1$ Hz), 1.74-1.82 (pentet, 2H, $J = 7.1$ Hz), 2.65 (s, 3H), 3.97-4.01 (t, 2H, $J = 6.6$ Hz), 6.74-6.76 (m, 2H), 8.04 (d, 1H, $J = 9.2$ Hz).

OC5 2MePh(mono3BrODBP). 4-Pentoxy-2-methylbenzoic acid (0.1107 g, 0.498 mmol) and 2-(4-hydroxy-3-bromophenyl)-5-(4-hydroxyphenyl)-1,3,4-oxadiazole (0.839 g, 0.252 mmol) were added with dimethylamino pyridine (DMAP) (0.0160 g, 0.131 mmol) and dry dichloromethane (15 mL) into a 100 mL round bottom flask under nitrogen. These were stirred and ethyl dimethylaminopropyl carbodiimide HCl (EDC HCl) (0.0977 g, 0.509 mmol) was added with more dry dichloromethane (5 mL). This solution was left stirring for three nights and checked for completion with TLC (eluent 2:1:1 hexanes-dichloromethane-acetone, $R_f = 0.79$). It was then worked up by adding DI water (20 mL) to the round bottom flask before being transferred to a 250 mL separatory funnel. Dichloromethane (20 mL) was added and the organic layer was washed with DI water (20 mL) and then 1M HCl. Some emulsion appeared between layers and a few mL of saturated NaCl were added. The aqueous washes were back extracted with fresh dichloromethane. The combined organic extracts were dried with $MgSO_4$, filtered, and then solvent was removed by rotary evaporation to yield a crude white powder. The product was purified by flash chromatography (eluent 20:10:1.5 dichloromethane-hexanes-ethyl acetate, $R_f = 0.35$) and then recrystallized from ethanol and a small amount of chloroform to give a white flaky powder (0.0370 g, 19.19%). ^{1}H-NMR (400 MHz, $CDCl_3$) δ 0.95 (t, 6H, $J = 7.2$ Hz, CH_3), 1.35-1.51 (m, 8H, CH_2CH_2), 1.79-1.86 (pentet, 4H, $J = 7.0$ Hz, CH_2), 2.67 (s, 6H, CH_3), 4.04 (t, 4H, $J = 6.6$ Hz, OCH_2), 6.81-6.85 (m, 4H, Ar), 7.4 (d, 2H, $J = 6.8$ Hz, Ar), 7.45 (d, 1H, $J = 8.4$, Ar), 8.15-8.23 (m, 4H, Ar), 8.29 (d, 1H, $J = 8.4$ Hz, Ar), 8.43 (s, 1H, Ar).

OC6 2MePh(mono3BrODBP). A procedure, workup, and purification that was identical to that of the OC5 target compound was used except with 4-hexyloxy-2-methyl benzoic acid (0.1323 g, 0.560 mmol), 2-(4-hydroxy-3-bromophenyl)-5-(4-hydroxyphenyl)-1,3,4-oxadiazole (0.0922 g, 0.277 mmol), DMAP (0.0180 g, 0.147 mmol), and EDC HCl (0.1117 g, 0.583 mmol). Completion was checked by TLC (eluent 2:1:1 hexanes-dichloromethane-acetone, $R_f = 0.8$), the product was purified using flash chromatography (eluent 20:10:1.5 dichloromethane-hexanes-ethyl acetate, $R_f = 0.35$), and recrystallized to give a flaky white powder (0.0541 g, 24.39%). ^{1}H-NMR (400 MHz, $CDCl_3$) δ 0.91 (t, 6H, $J = 6.4$ Hz, CH_3), 1.35-1.37 (m, 8H, CH_2CH_2), 1.47 (pentet, 4H, $J = 7.2$ Hz, CH_2), 1.81 (pentet, 4H, $J = 7.0$ Hz, CH_2), 2.67 (s, 6H, CH_3), 4.04 (t, 4H, $J = 6.2$ Hz, OCH_2), 6.81-6.85 (m, 4H, Ar), 7.40 (d, 2H, $J = 7.6$ Hz, Ar) 7.44 (d, 1H, $J = 8.4$ Hz, Ar), 8.15-8.22 (m, 4H, Ar), 8.28 (d, 1H, $J = 8.4$ Hz, Ar), 8.44 (s, 1H, Ar).

OC7 2MePh(mono3BrODBP). Procedure, workup, and purification identical to OC5 target

compound except using 4-heptyloxy-2-methyl benzoic acid (0.1228 g, 0.491 mmol), 2-(4-hydroxy-3-bromophenyl)-5-(4-hydroxyphenyl)-1,3,4-oxadiazole (0.0836 g, 0.251 mmol), DMAP (0.0159 g, 0.130 mmol), and EDC HCl (0.0966 g, 0.504 mmol). It was checked for completion by TLC (eluent 2:1:1 hexanes-dichloromethane-acetone, $R_f = 0.78$), purified by flash chromatography (eluent 20:10:1.5 dichloromethane-hexanes-ethyl acetate, $R_f = 0.56$), and recrystallized to give yielded flaky white powder (0.0375 g, 18.42%). ^{1}H-NMR (400 MHz, $CDCl_3$) δ 0.90 (t, 6H, *J* = 6.0 Hz, C*H*$_3$), 1.32-1.39 (m, 12H, C*H*$_2$C*H*$_2$C*H*$_2$), 1.45-1.49 (pentet, 4H, *J* = 7.6 Hz, C*H*$_2$), 1.80-1.83 (pentet, 4H, 6.8 Hz, C*H*$_2$), 2.67 (s, 6H, C*H*$_3$), 4.03 (t, 4H, *J* = 6.8 Hz, OC*H*$_2$), 6.81-6.85 (m, 4H, Ar), 7.40 (d, 2H, *J* = 7.2 Hz, Ar), 7.45 (d, 1H, *J* = 8.8 Hz, Ar), 8.15-8.23 (m, 4H, Ar), 8.28 (d, 1H, *J* = 8.0 Hz, Ar), 8.44 (s, 1H, Ar).

OC8 2MePh(mono3BrODBP). Procedure, workup, and purification identical to OC5 target compound except using 4-octoxy-2-methyl benzoic acid (0.1562 g, 0.591 mmol), 2-(4-hydroxy-3-bromophenyl)-5-(4-hydroxyphenyl)-1,3,4-oxadiazole (0.0981 g, 0.294 mmol), DMAP (0.0197 g, 0.161 mmol), and EDC (0.1195 g, 0.623 mmol). Compound was checked for completion by TLC (eluent 2:1:1 hexanes-dichloromethane-acetone, $R_f = 0.68$), purified by flash chromatography (eluent 20:10:1.5 dichloromethane-hexanes-ethyl acetate, $R_f = 0.65$), and recrystallized to yield a flaky white powder (0.0808 g, 32.00%). ^{1}H-NMR (400 MHz, $CDCl_3$) δ 0.89 (t, 6H, *J* = 6.8 Hz, C*H*$_3$), 1.29-1.35 (m, 16H, C*H*$_2$C*H*$_2$C*H*$_2$C*H*$_2$), 1.43-1.51 (pentet, 4H, *J* = 7.3 Hz, C*H*$_2$), 1.78-1.85 (pentet, 4H, *J* = 7.1 Hz, C*H*$_2$), 2.67 (s, 6H, C*H*$_3$), 4.04 (t, 4H, *J* = 4.4 Hz, OC*H*$_2$), 6.81-6.85 (m, 4H, Ar), 7.40 (d, 2H, *J* = 8.8 Hz, Ar), 7.44 (d, 1H, *J* = 8.4, Ar), 8.15-8.23 (m, 4H, Ar), 8.28 (d, 1H, *J* = 8.4 Hz, Ar), 8.44 (s, 1H, Ar).

OC9 2MePh(mono3BrODBP). Procedure, workup, and purification identical to OC5 target compound except using 4-nonoxy-2-methyl benzoic acid (0.1117 g, 0.402 mmol), 2-(4-hydroxy-3-bromophenyl)-5-(4-hydroxyphenyl)-1,3,4-oxadiazole (0.0667 g, 0.201 mmol), DMAP (0.0133 g, 0.109 mmol), and EDC (0.0817 g, 0.426 mmol). Compound was checked for completion by TLC (eluent 2:1:1 hexanes-dichrolomethane-acetone, $R_f = 0.84$), purified by flash chromatography (eluent 20:10:1.5 dichloromethane-hexanes-ethyl acetate, $R_f = 0.33$), and recrystallized to yield flaky white powder (0.0362 g, 20.59%). ^{1}H-NMR (400 MHz, $CDCl_3$) δ 0.88 (t, 6H, *J* = 6.2 Hz, C*H*$_3$), 1.29-1.38 (m, 20H, C*H*$_2$C*H*$_2$C*H*$_2$C*H*$_2$C*H*$_2$), 1.43-1.51 (pentet, 4H, *J* = 7.2 Hz, C*H*$_2$), 1.78-1.85 (pentet, 4H, *J* = 7.1 Hz, C*H*$_2$), 2.67 (s, 6H, C*H*$_3$), 4.03 (t, 4H, *J* = 6.4 Hz, OC*H*$_2$), 6.81-6.85 (m, 4H, Ar), 7.40 (d, 2H, *J* = 8.8 Hz, Ar), 7.45 (d, 1H, *J* = 8.0, Ar), 8.15-8.23 (m, 4H, Ar), 8.28 (d, 1H, *J* = 8.0 Hz, Ar), 8.40 (s, 1H, Ar).

OC10 2MePh(mono3BrODBP). Procedure, workup, and purification identical to OC5 target compound except using 4-decyloxy-2-methyl benzoic acid (0.1527 g, 0.523 mmol), 2-(4-hydroxy-3-bromophenyl)-5-(4-hydroxyphenyl)-1,3,4-oxadiazole (0.0893 g, 0.261 mmol), DMAP (0.0174 g, 0.131 mmol), and EDC HCl (0.1058 g, 0.538 mmol). Compound was checked for completion by TLC (eluent 2:1:1 hexanes-dichrolomethane-acetone, $R_f = 0.78$), purified by flash chromatography (eluent 20:10:1.5 dichloromethane-hexanes-ethyl acetate, $R_f = 0.75$), and recrystallized to yield flaky white powder (0.1111 g, 45.38%). ^{1}H-NMR (400 MHz, $CDCl_3$) δ 0.88 (t, 6H, *J* = 6.8 Hz, C*H*$_3$), 1.27-1.38 (m, 24H, C*H*$_2$C*H*$_2$C*H*$_2$C*H*$_2$C*H*$_2$C*H*$_2$), 1.43-1.51 (pentet, 4H, *J* = 7.4 Hz, C*H*$_2$), 1.78-1.85 (pentet, 4H, *J* = 7.0 Hz, C*H*$_2$), 2.67 (s, 6H, C*H*$_3$), 4.03 (t, 4H, *J* = 6.4 Hz, OC*H*$_2$), 6.81-6.85 (m, 4H, Ar), 7.39 (d, 2H, *J* = 8.8 Hz, Ar), 7.44 (d, 1H, *J* = 8.4, Ar), 8.15-8.23 (m, 4H, Ar), 8.28 (d, 1H, *J* = 8.4 Hz, Ar), 8.44 (s, 1H, Ar).

References

[1] Taken from Case Western Reserve University's Polymers and Liquid Crystal Virtual textbook. Case Western Reserve University. http://plc.cwru.edu/tutorial/enhanced/files/textbook.htm

[2] Freiser, M.J.; *phys. Rev. Lett.;* **1970**, 24, 1041.

[3] Photinos, D. J.; Tschierske, C.; *J. Mater. Chem*., **2010**, 20, 4263.

[4] Dingemans, T.J.; Madsen, L.A.; Nakata, M.; Samulski, E.T.; *Phys. Rev. Lett.* **2004**, 92,12.

[5] Acharya, B.; Kumar, S.; Primak, A.; *Phys. Rev. Lett.* **2004**, 92, 145506-1-145506-4.

[6] Cho, J. S.; Lee, G. S.; Kim, J. C.; Shin, S. T.; Yoon, T.-H.; *J. Appl. Phys*., **2009**, 105, 094509.

[7] Apreutesei, D.; Mehl, G. H.; *J. Mater. Chem*., **2007**, 17, 4711.

[8] Goodby, J. W.; Gortz, V.; *Chem. Commun*., **2005**, 3262.

[9] Cooper, L.L.; Scharrer, E.; Samulski, E.T.; *Mol. Cryst. Liq. Cryst.* **2009**, 511, 203-217.

[10] Scharrer, E.; Speetjens, F.; Lindborg, J.; Tauscher, T.; LaFemina, N.; Nguyen, J.; Samulski, E.; Vita, F.; Francescangeli, O; *J. Mater. Chem.,* **2012**, 22, 22558

Appendix

DSC Figures

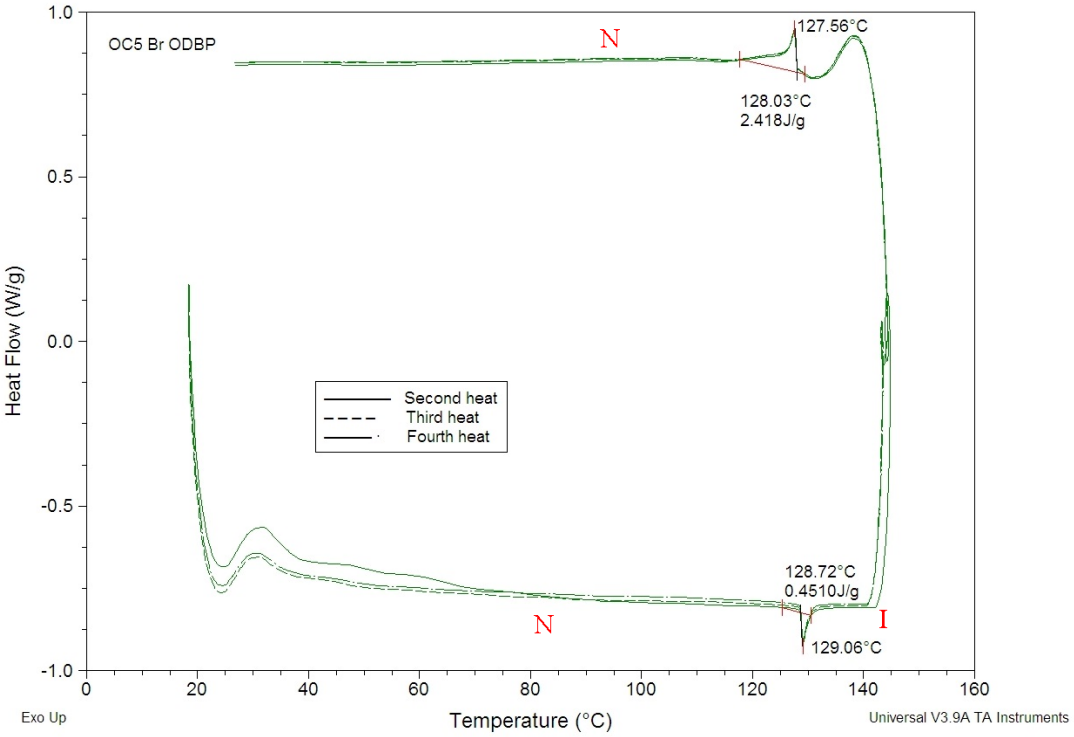

Figure 7b. DSC thermogram of OC5 subsequent heats.

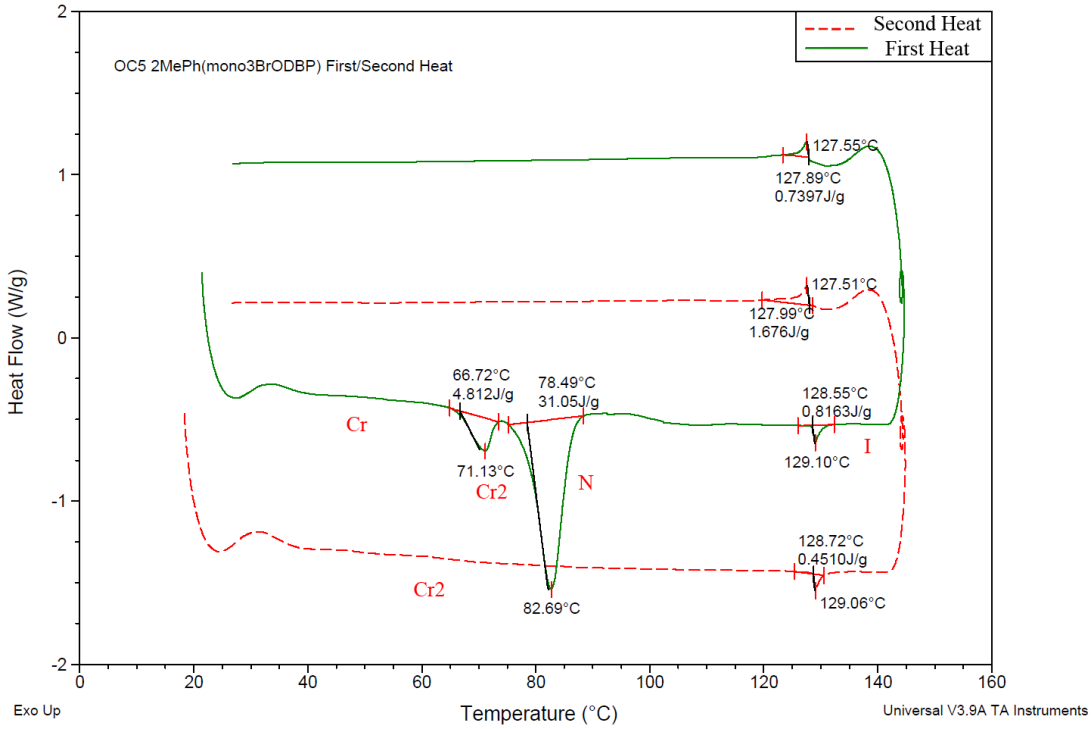

Figure 7c. DSC thermogram of OC5 first and second heats.

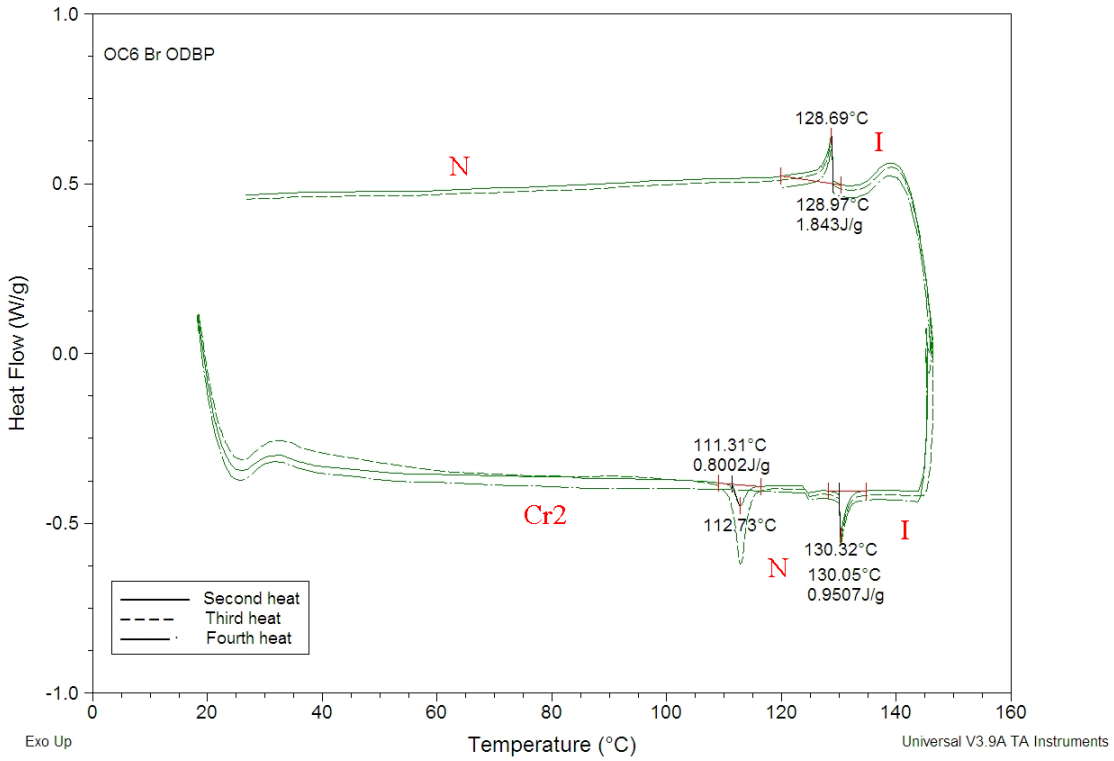

Figure 9c. DSC thermogram of OC6 subsequent heats.

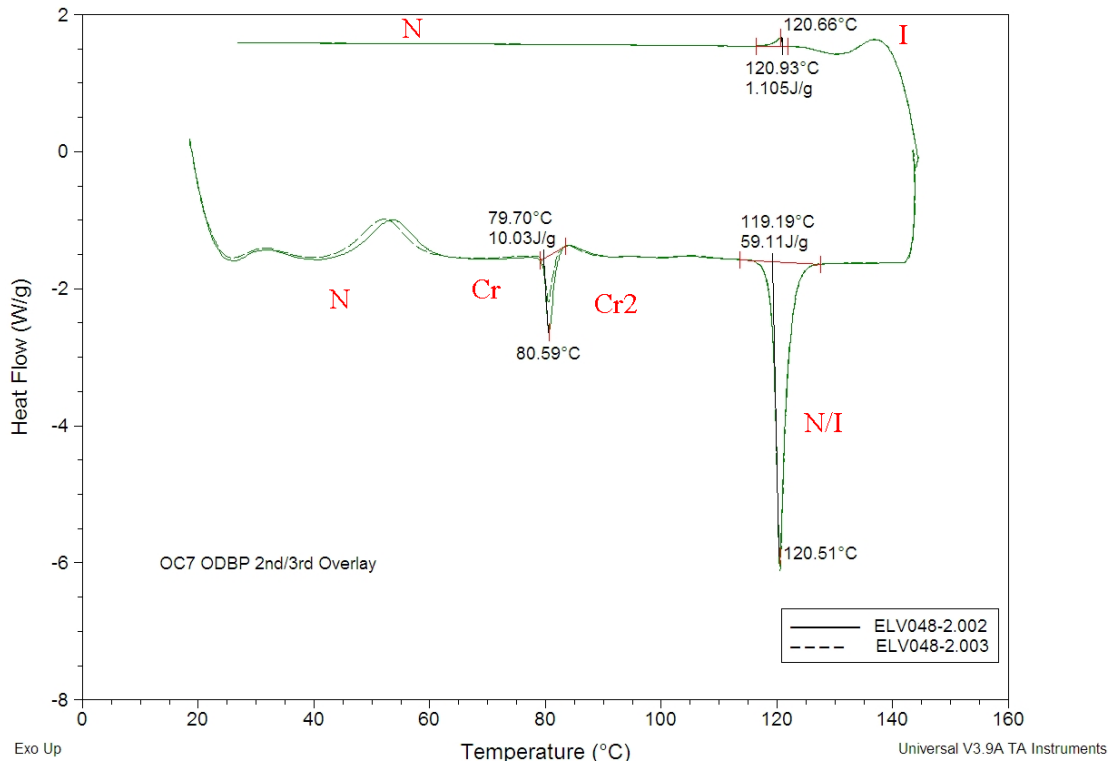

Figure 11c. DSC thermogram of OC7 subsequent heats.

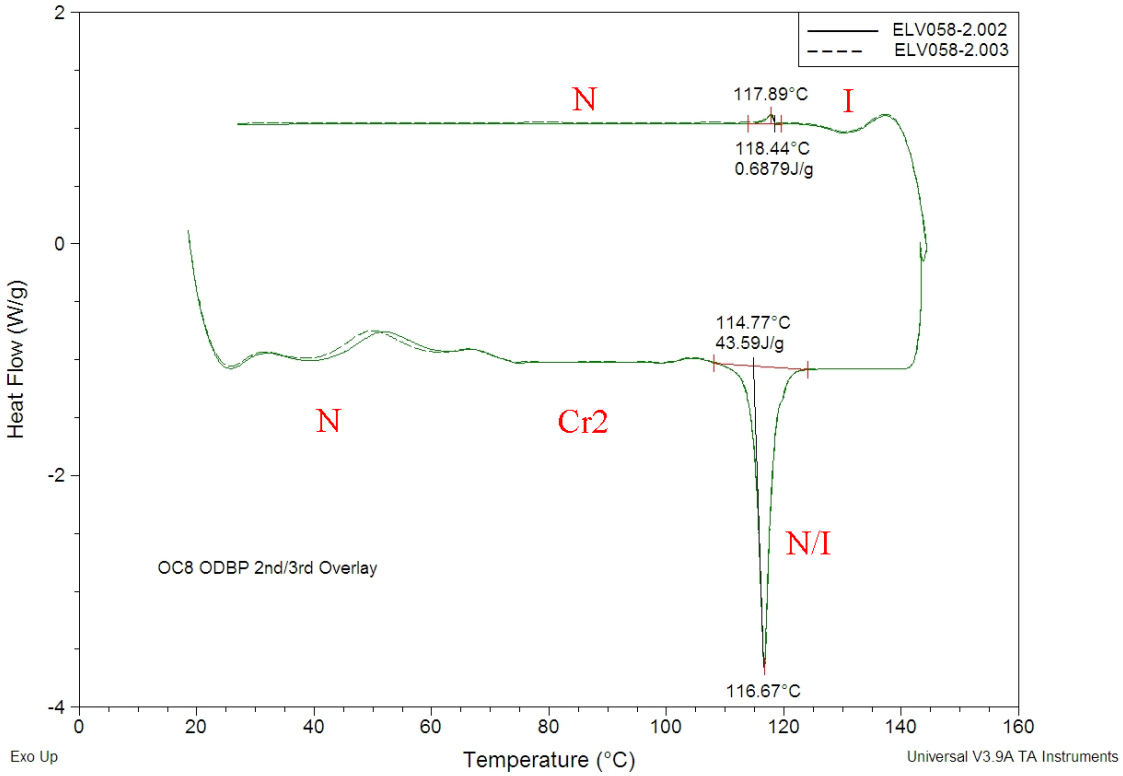

Figure 13b. DSC thermogram of OC8 subsequent heats.

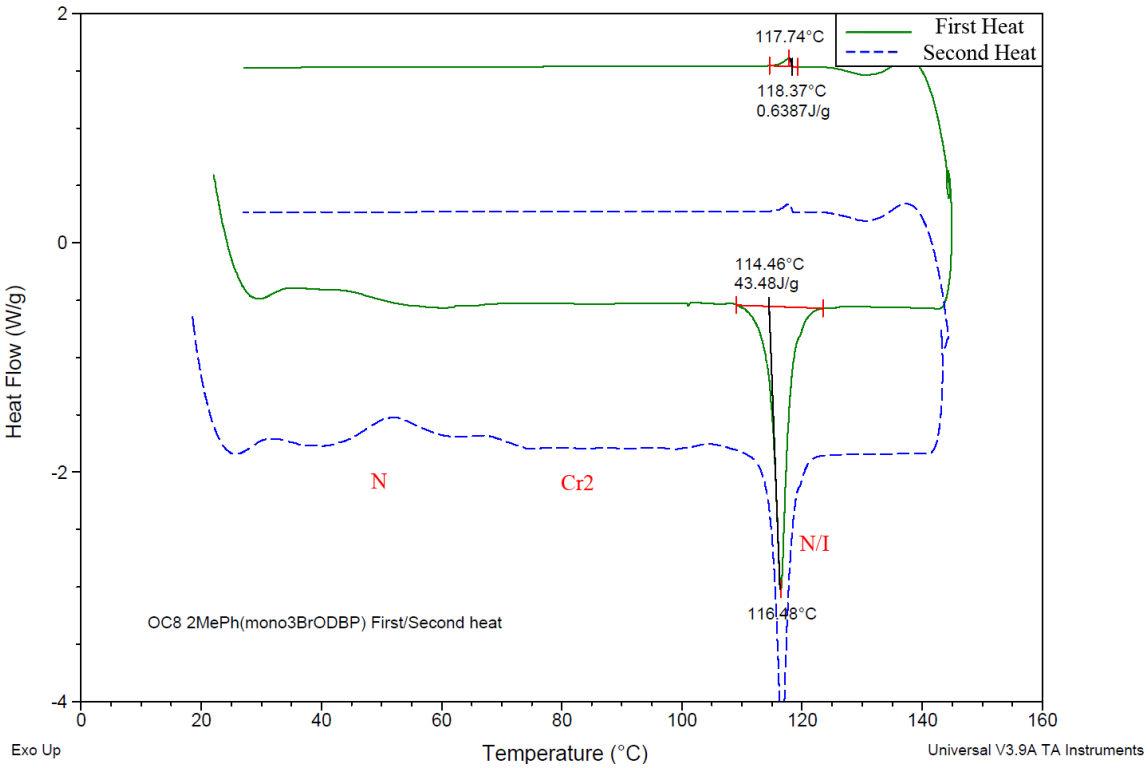

Figure 13c. DSC thermogram of OC8 first and second heats.

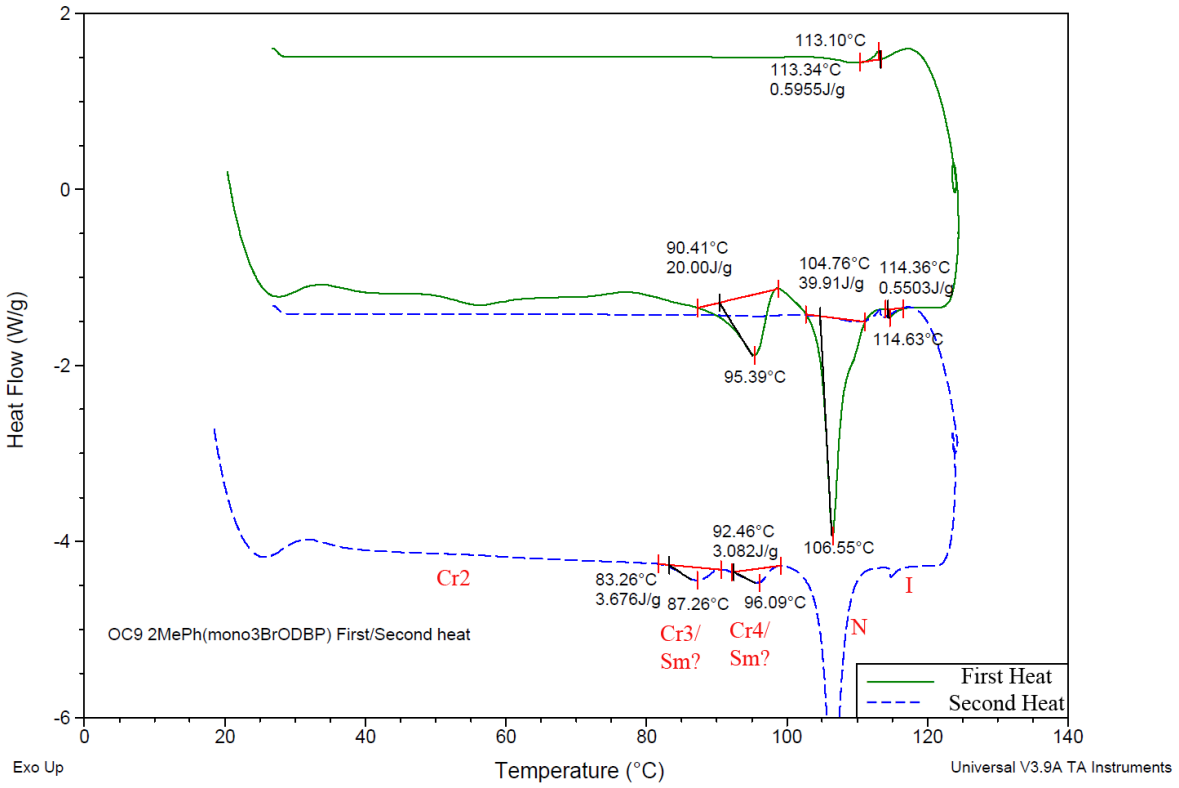

Figure 15c. DSC thermogram of OC9 first and second heats.

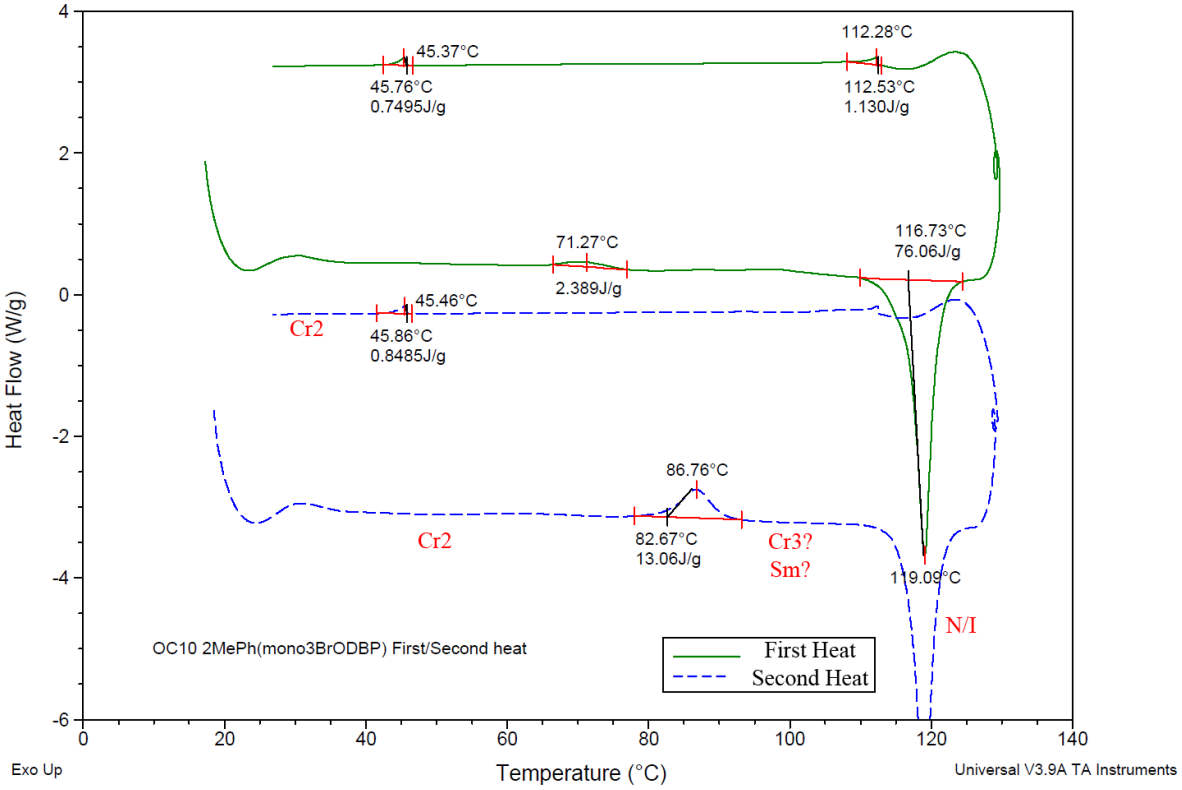

Figure 17c. DSC thermogram of OC10 first and second heats.

[1]H-NMR Spectra

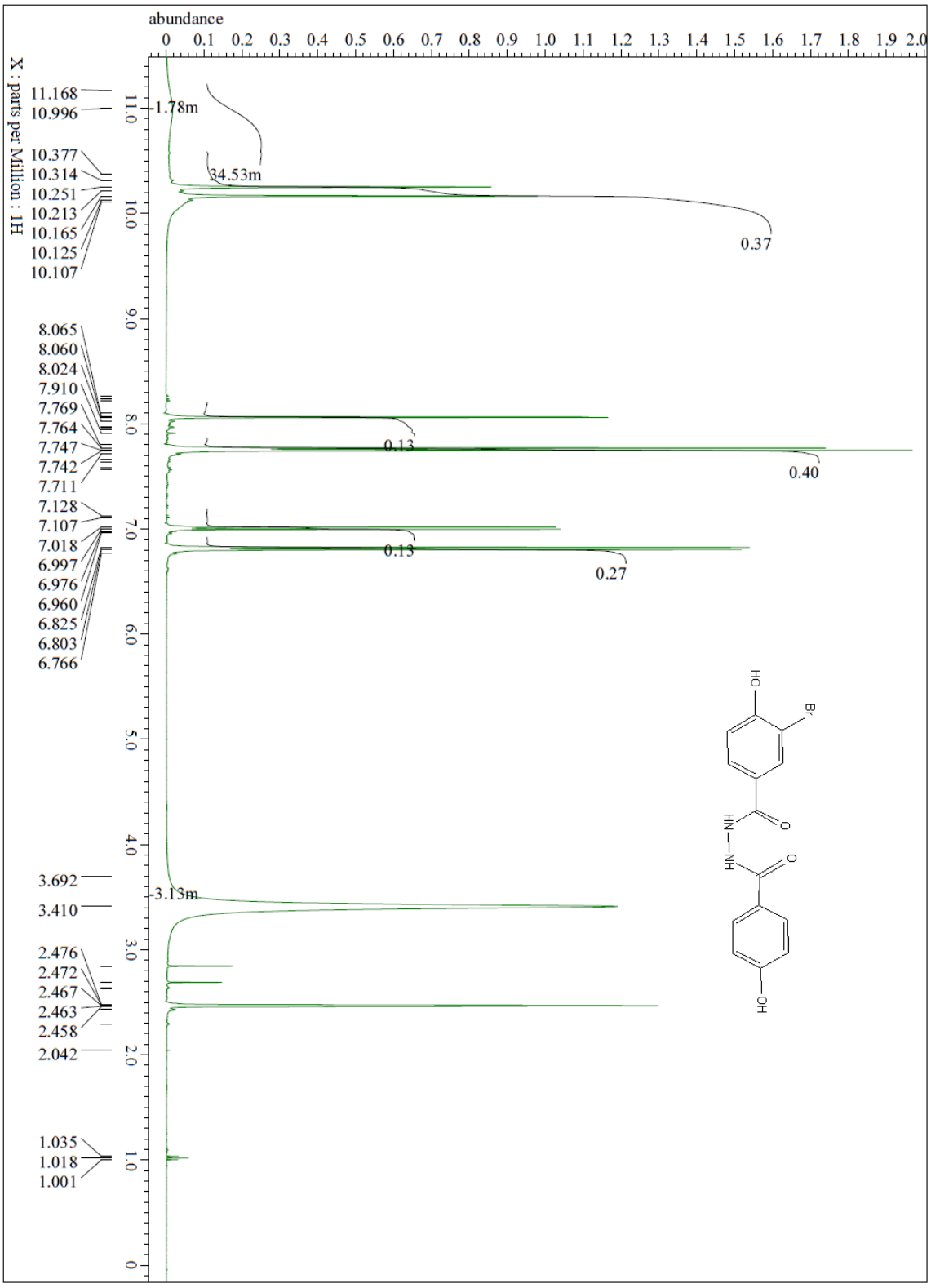

Figure 19. H-NMR spectrum of 4-Hydroxy-3-bromo-*N*-(4-hydroxybenzoyl) benzhydrazide.

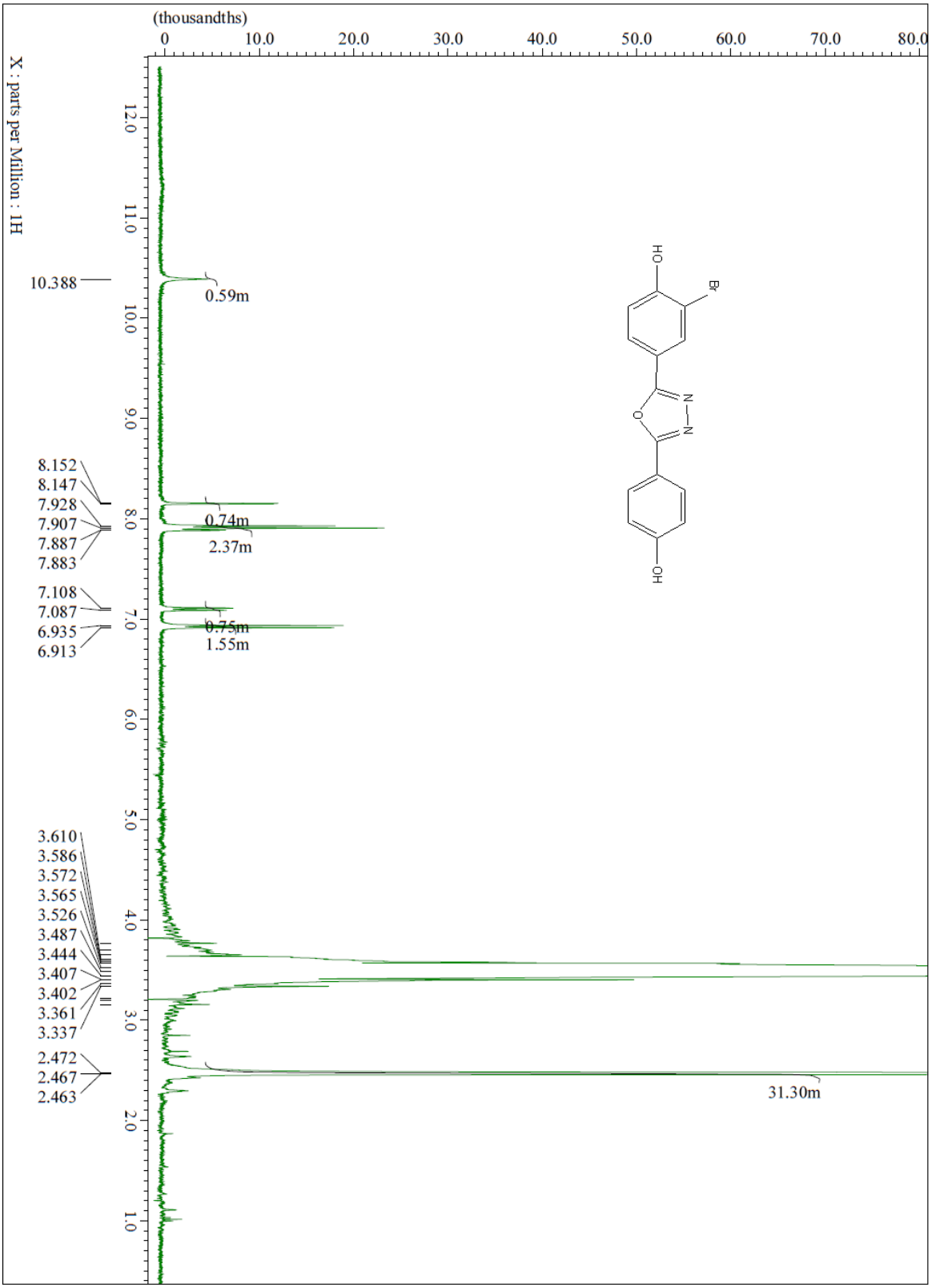

Figure 20. H-NMR spectrum of 2-(4-Hydroxy-3-bromophenyl)-5-(4-hydroxyphenyl)-1,3,4-oxadiazole.

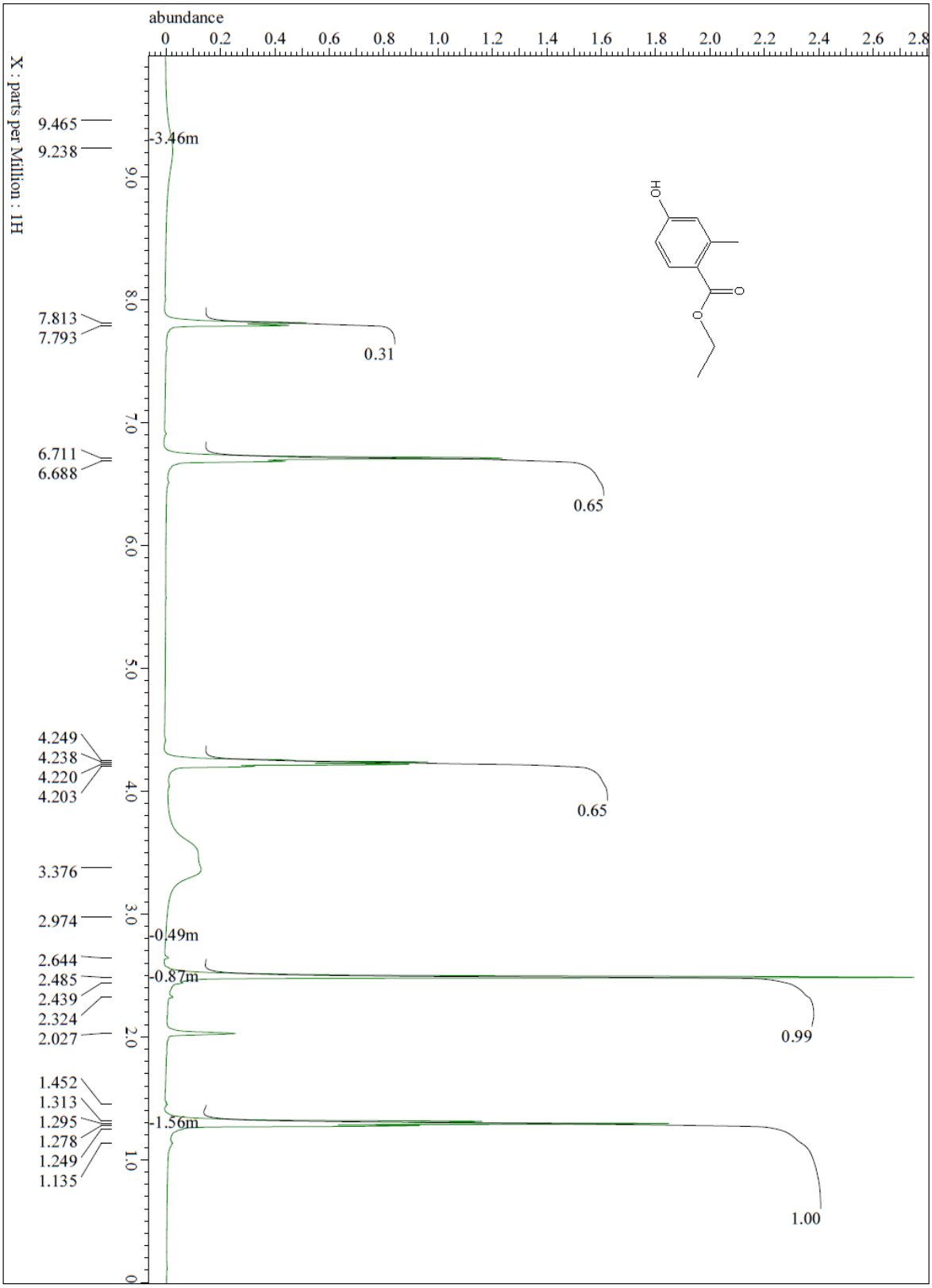

Figure 21. H-NMR spectrum of Ethyl 4-hydroxy-2-methyl benzoate.

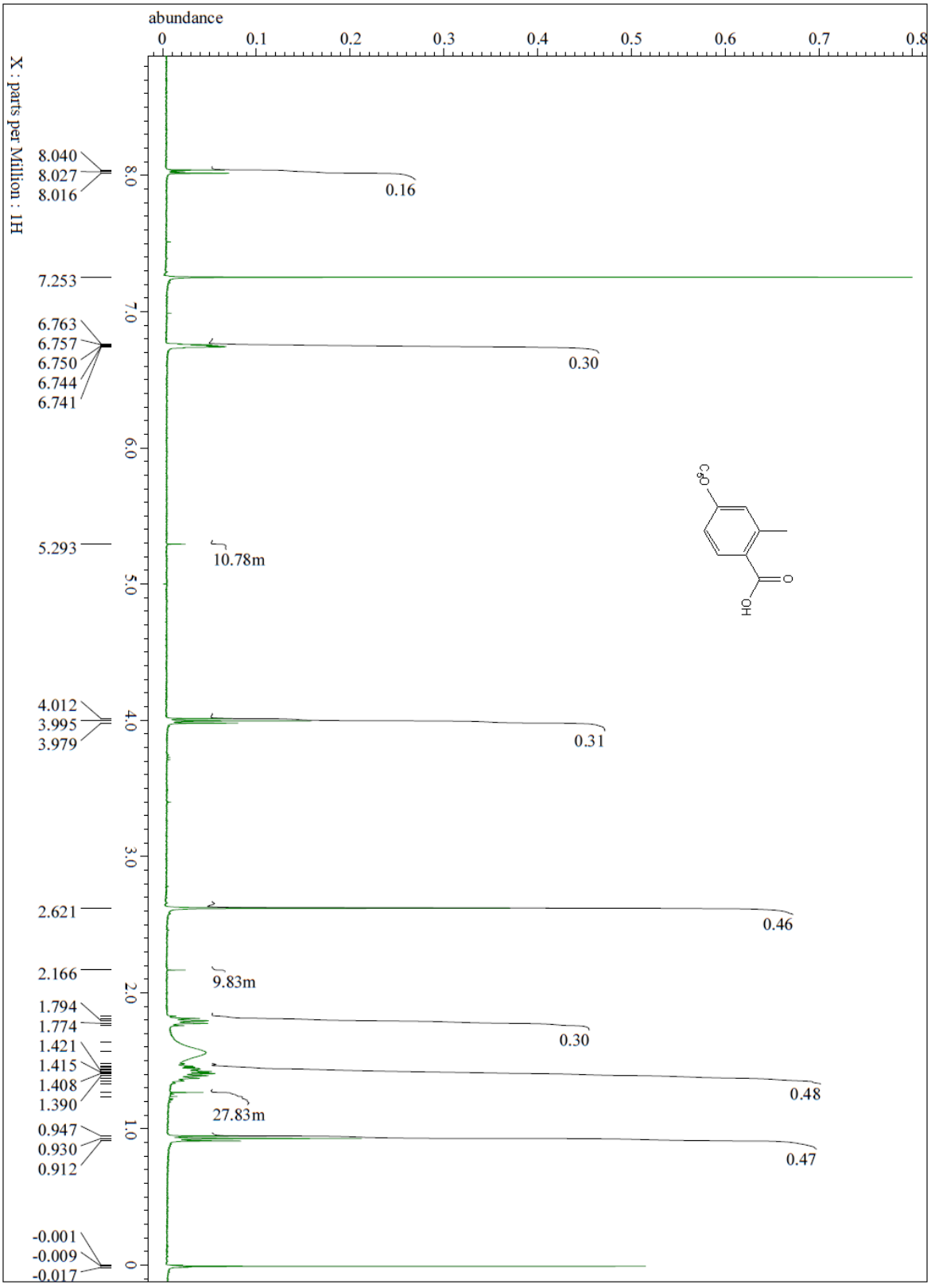

Figure 22. H-NMR spectrum of 4-pentoxy-2-methyl benzoic acid.

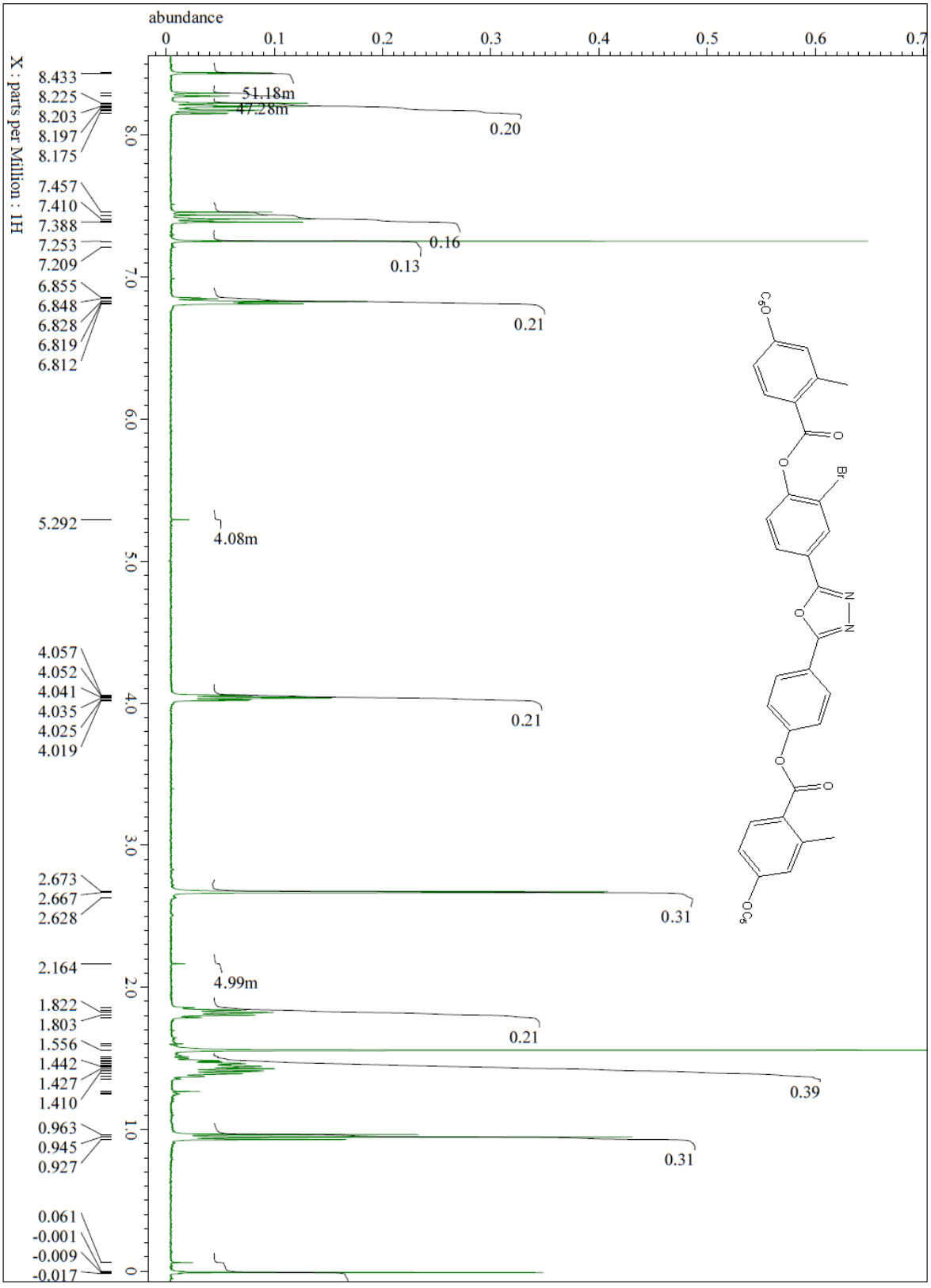

Figure 23. H-NMR spectrum of OC5 2MePh(mono3BrODBP).

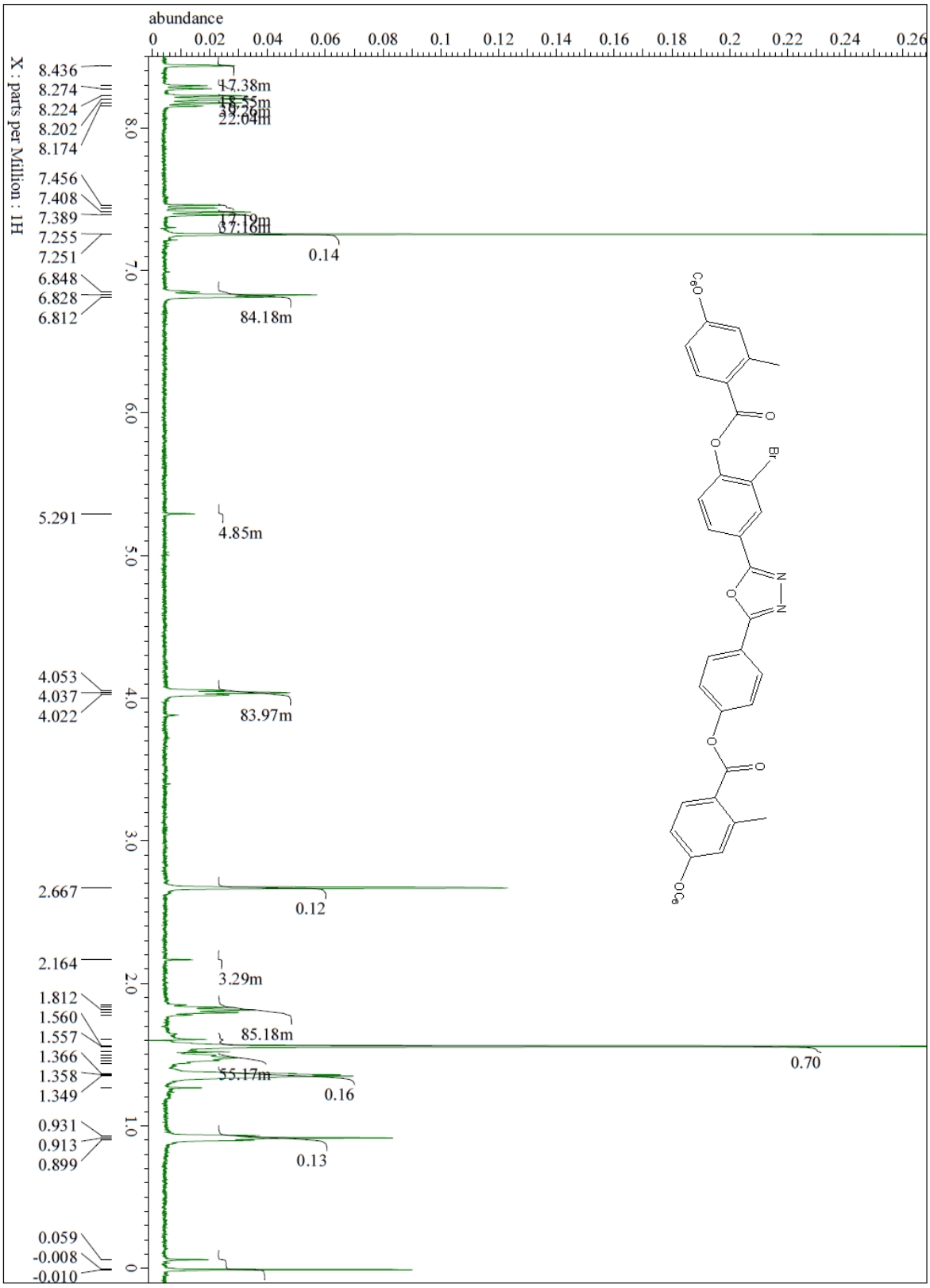

Figure 24. H-NMR spectrum of OC6 2MePh(mono3BrODBP).

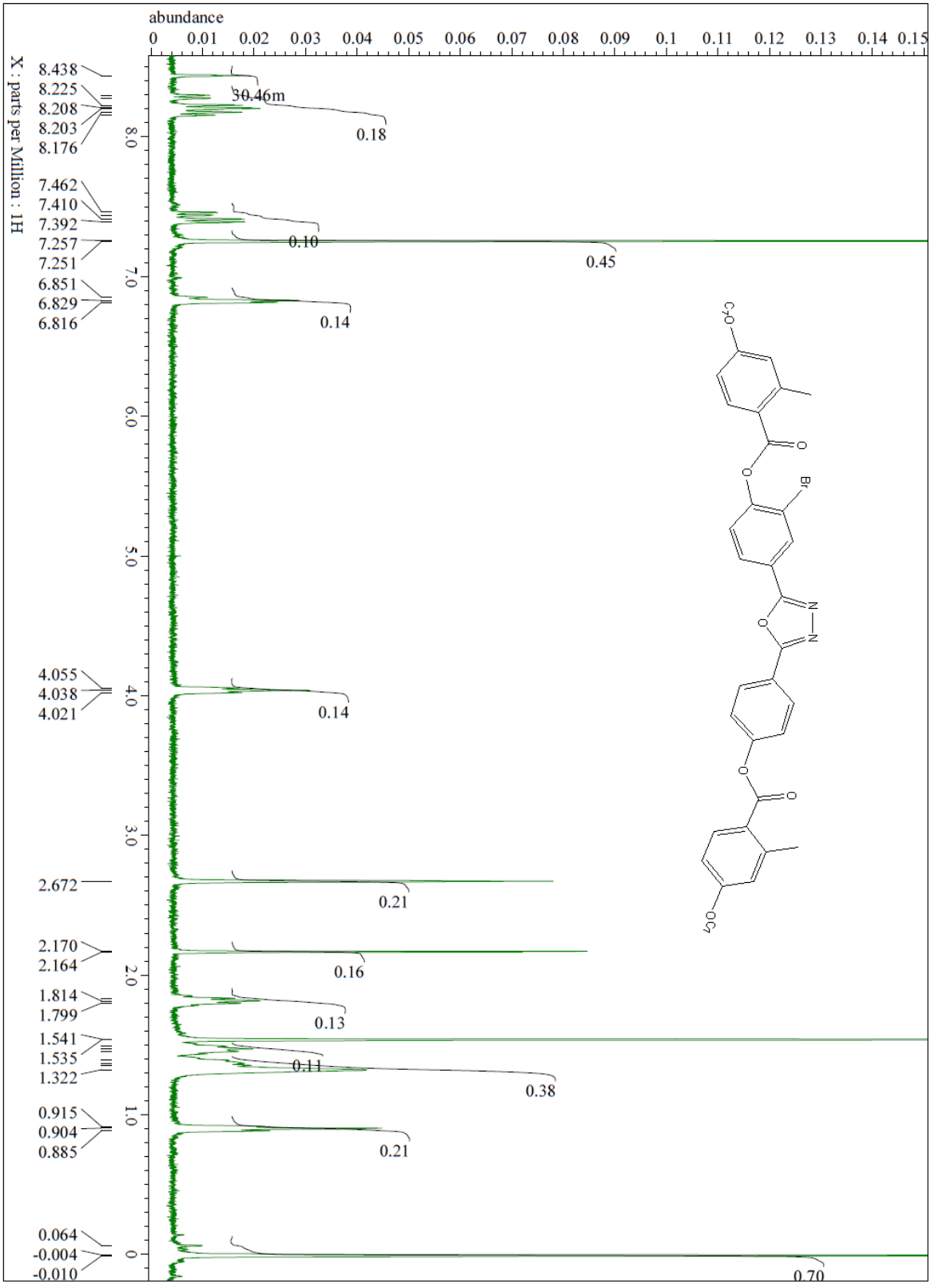

Figure 25. H-NMR spectrum of OC7 2MePh(mono3BrODBP).

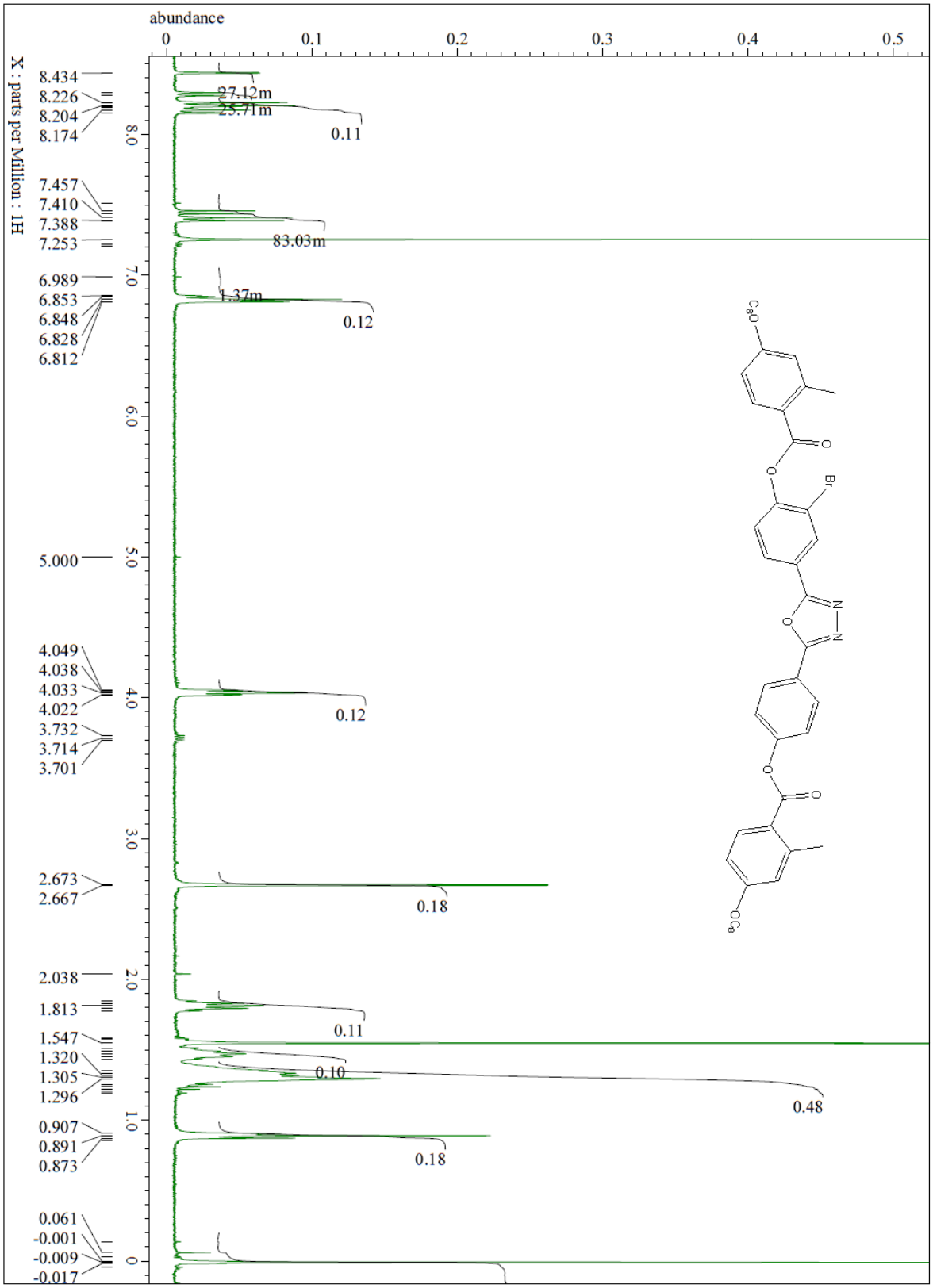

Figure 26. H-NMR spectrum of OC8 2MePh(mono3BrODBP).

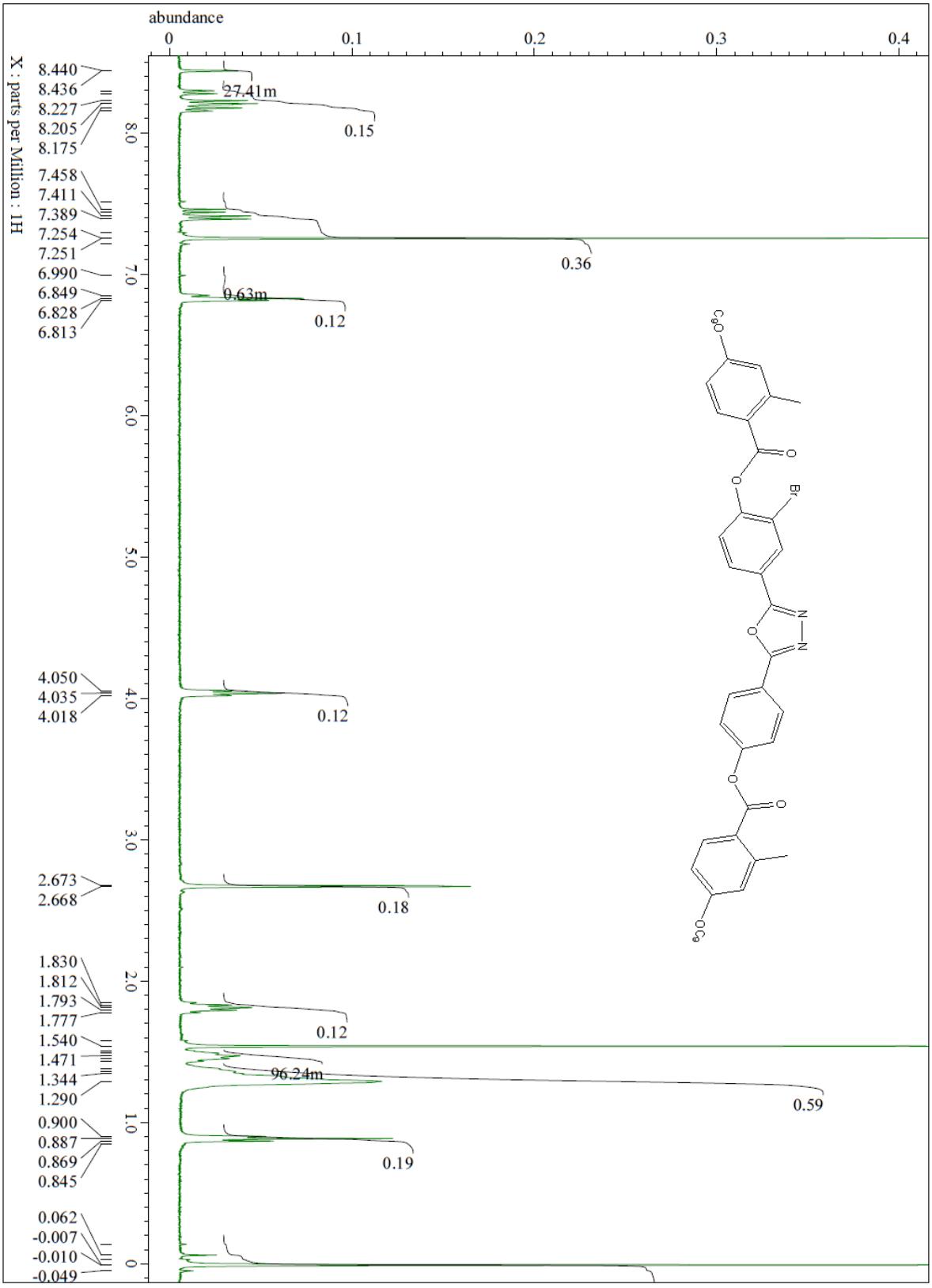

Figure 27. H-NMR spectrum of OC9 2MePh(mono3BrODBP).

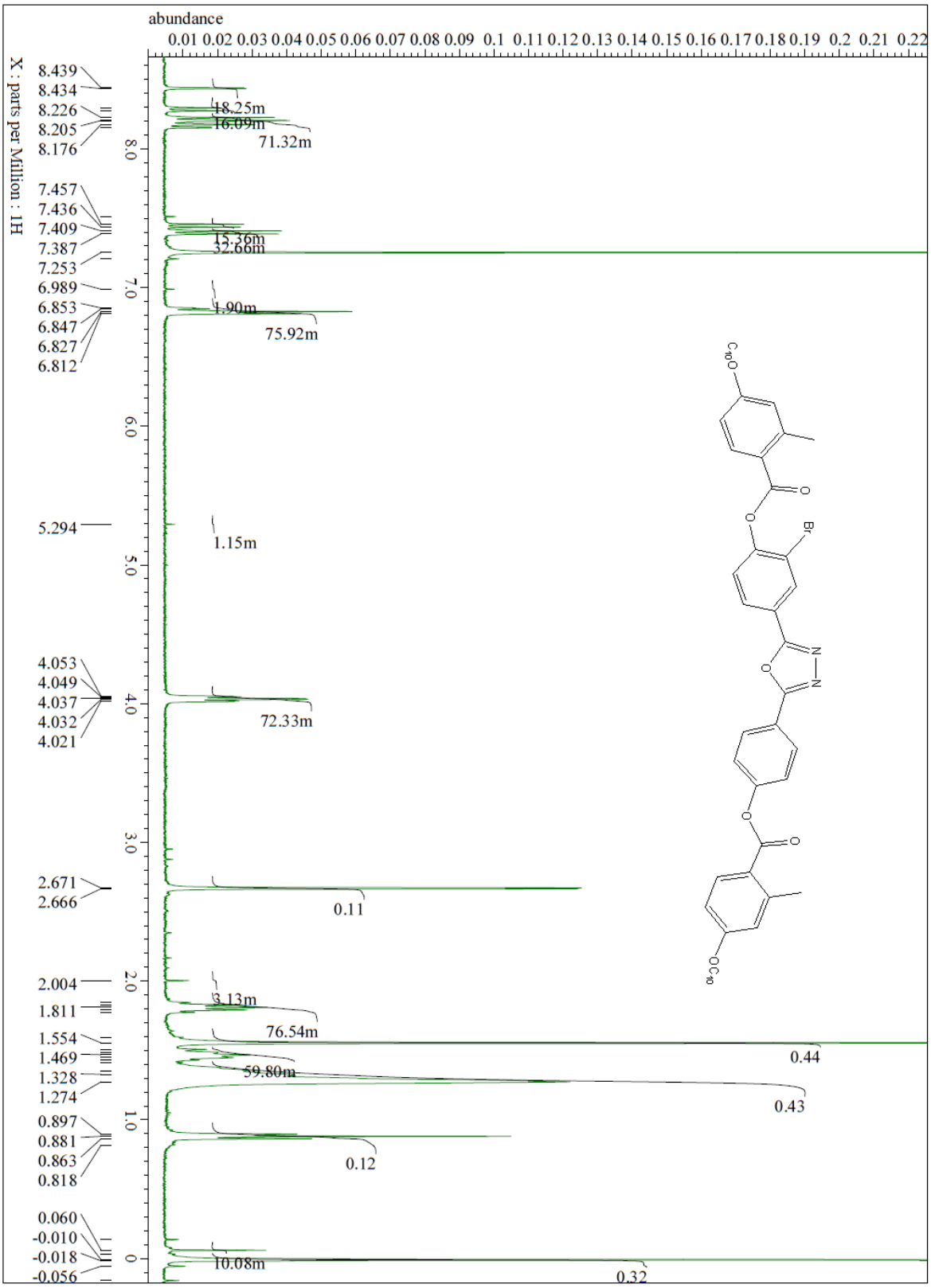

Figure 28. H-NMR spectrum of OC10 2MePh(mono3BrODBP).